Photosynthesis Research (2024) 159:97–114
https://doi.org/10.1007/s11120-023-01019-9

RESEARCH

Roles of ApcD and orange carotenoid protein in photoinduction of electron transport upon dark–light transition in the *Synechocystis* PCC 6803 mutant deficient in flavodiiron protein Flv1

Irina V. Elanskaya[1] · Alexander A. Bulychev[2] · Evgeny P. Lukashev[2] · Elena M. Muronets[1] · Eugene G. Maksimov[2]

Received: 31 December 2022 / Accepted: 13 April 2023 / Published online: 24 April 2023

Abstract

Flavodiiron proteins Flv1/Flv3 accept electrons from photosystem (PS) I. In this work we investigated light adaptation mechanisms of Flv1-deficient mutant of *Synechocystis* PCC 6803, incapable to form the Flv1/Flv3 heterodimer. First seconds of dark–light transition were studied by parallel measurements of light-induced changes in chlorophyll fluorescence, P700 redox transformations, fluorescence emission at 77 K, and OCP-dependent fluorescence quenching. During the period of Calvin cycle activation upon dark–light transition, the linear electron transport (LET) in wild type is supported by the Flv1/Flv3 heterodimer, whereas in Δ*flv1* mutant activation of LET upon illumination is preceded by cyclic electron flow that maintains State 2. The State 2–State 1 transition and Orange Carotenoid Protein (OCP)-dependent non-photochemical quenching occur independently of each other, begin in about 10 s after the illumination of the cells and are accompanied by a short-term re-reduction of the PSI reaction center ($P700^+$). ApcD is important for the State 2–State 1 transition in the Δ*flv1* mutant, but S-M rise in chlorophyll fluorescence was not completely inhibited in Δ*flv1*/Δ*apcD* mutant. LET in Δ*flv1* mutant starts earlier than the S–M rise in chlorophyll fluorescence, and the oxidation of plastoquinol (PQH_2) pool promotes the activation of PSII, transient re-reduction of $P700^+$ and transition to State 1. An attempt to induce state transition in the wild type under high intensity light using methyl viologen, highly oxidizing P700 and PQH_2, was unsuccessful, showing that oxidation of intersystem electron-transport carriers might be insufficient for the induction of State 2–State 1 transition in wild type of *Synechocystis* under high light.

Keywords *Synechocystis* PCC 6803 · Dark–light transition · State transitions · Chlorophyll fluorescence induction · P700 redox changes · Non-photochemical quenching · Orange carotenoid protein- deficient mutant · Flavodiiron protein Flv1-deficient mutant · ApcD-deficient mutant · Methyl viologen

Abbreviations

CET	Cyclic electron transport
Chl	Chlorophyll
DBMIB	2,5-Dibromo-6-isipropyl-3-methyl-1,4-benzoquinone
DCMU	3-(3,4-Dichlorophenyl)-1,1-dimethylurea
ETC	Electron transport chain
FDP(s)	Flavodiiron protein(s)
FR	Far-red (light)
HL	High intensity light
LET	Linear electron transport
LL	Low intensity light
MV	Methyl viologen
NPQ	Non-photochemical quenching of excitation
P700	Donor pigment of PSI
PBS	Phycobilisomes
PQ	Plastoquinone
PSI and PSII	Photosystems I and II
PSA	Photosynthetic apparatus
Rubisco	Ribulose 1,5-bisphosphate carboxylase-oxygenase
WL	White light
WT	Wild type

✉ Eugene G. Maksimov
emaksimoff@yandex.ru

[1] Department of Genetics, Faculty of Biology, Lomonosov Moscow State University, Moscow 119991, Russia

[2] Department of Biophysics, Faculty of Biology, Lomonosov Moscow State University, Moscow 119991, Russia

Introduction

In the thylakoid membrane of cyanobacteria, two main modes of photosynthetic electron transport can occur. In linear electron transport (LET), electrons are transferred from the water splitting site at photosystem II (PSII) to PSI via plastoquinone (PQ), cytochrome b_6f complex (Cyt*b6f*), and plastocyanin (PC). At the acceptor side of PSI, ferredoxin (Fd) reduced on excitation of photosystem I (PSI) mediates electron transfer from PSI to $NADP^+$ via Fd:$NADP^+$ reductase (FNR). In the cyclic electron transport (CET), PSI can be re-reduced by recycling electrons from Fd to the PQ pool, mostly via NDH-1 complex (Miller and Vaughn 2021). Despite the fact that cyanobacterial NDH-1 is an analog of respiratory complex I that oxidizes NAD(P)H, the most likely electron donor for NDH-1 in cyanobacteria is ferredoxin (Gao et al. 2016; Schuller et al. 2019). Both LET and CET reactions are coupled with proton pumping across the thylakoid membrane, and the resulting electrochemical proton gradient drives the H^+-ATP synthase to produce ATP, but CET generates the proton motive force without net accumulation of NADPH (Bendall and Manasse 1995; Munekage et al. 2004; Peltier et al. 2016; Yamori and Shikanai 2016). While LET is responsible for the bulk of light-induced proton pumping, CET via NDH-1 is capable of generating about 40% of the proton pumping rate when LET is inactivated (Miller and Vaughn 2021). In the dark, the intersystem electron transport chain (ETC) of photosynthesis (PQ, Cyt*b6f,* and PC) can be reduced by electron fluxes from the respiratory dehydrogenases and oxidized by cytochrome *c*- and quinol oxidases (Ermakova et al. 2016; Fork and Satoh 1983; Mullineaux and Allen 1990).

ATP and NADPH generated by light reactions are utilized primarily for assimilation of carbon dioxide in the Calvin cycle. However, the Calvin cycle reactions are not functional in the dark. Both in chloroplasts and cyanobacteria, two enzymes of the Calvin cycle, phosphoribulokinase and glyceraldehyde-3-phosphate dehydrogenase undergo dark/light regulation through the formation/dissociation of a multiprotein complex mediated by a small, so-called, intrinsically disordered protein, CP12 (Tamoi and Shigeoka 2015). Upon exposing dark-acclimated cells to light, a rapid increase in effective absorption cross section of PSII occurs, accompanied by enhanced electron flow (Gerotto et al. 2016; Yamori 2016).

Delayed activation of the Calvin cycle results in a strong acceptor side limitation in PSI and over-reduction of PSI reaction centers (Huang et al. 2018, 2019a, b; Wada et al. 2018; Yamamoto et al. 2016). In cyanobacteria, algae and nonflowering plants, this over-reduction of PSI reaction centers is rapidly relieved by flavodiiron proteins (FDPs) that act as strong electron sinks downstream of PSI, providing for electron outflow from PSI to O_2 without production of reactive oxygen species (Huang et al. 2019b; Ilík et al. 2017; Jokel et al. 2018). The absence of FDPs in dark-acclimated angiosperms is compensated by the higher level of CET around PSI, while the FDP-dependent reaction dominates over CET in gymnosperms (Noridomi et al. 2017). In the cyanobacterium *Synechocystis* PCC 6803 (hereafter *Synechocystis*) the heterodimer of flavodiiron proteins Flv1/Flv3 mediates the Mehler-like reaction (Allahverdiyeva et al. 2013; Gerotto et al. 2016; Helman et al. 2003; Vicente et al. 2002), which is important for survival of cyanobacteria under fluctuating light (Allahverdiyeva et al. 2015, 2013). Cyanobacterial Flv proteins contain NAD(P)H:flavin oxidoreductase C-terminal module, which was proposed to facilitate O_2 reduction to H_2O with NAD(P)H as an electron donor (Allahverdiyeva et al. 2015; Vicente et al. 2002). However, a number of data pointed to the possible role of Fd as an electron donor to Flv proteins (Battchikova et al. 2011; Hanke et al. 2011; Nikkanen et al. 2020; Peden et al. 2013), and it has been shown that when the Calvin cycle is inactive, ferredoxin is the most likely Flv1/Flv3 partner in *Synechocystis* (Sétif et al. 2020).

To increase the probability of light absorption and capture of electron excitation energy by photosystems, cyanobacteria use water-soluble light-collecting complexes, phycobilisomes (PBSs), located at the outer surface of the thylakoid membrane. PBS in *Synechocystis* consists of three core cylinders which include allophycocyanin discs stacked next to each other and radiating out of the core peripheral rods composed of phycocyanin. Two basal cylinders are arranged anti-parallel and lie directly onto the thylakoid membrane. The third cylinder is located on the stromal side above the two cylinders (Arteni et al. 2009; Glazer 1984). Light energy collected by phycocyanin in the peripheral rods is transferred to chlorophyll *a* in reaction centers of PSI and PSII via the terminal energy acceptors of the phycobilisome, ApcD, ApcF, and ApcE (Adir et al. 2020).

For optimal photosynthesis, cyanobacteria have developed a number of mechanisms, which include acclimation of light harvesting to different spectra of illumination (state transitions) (Mullineaux and Allen 1990) and the Orange Carotenoid-binding Protein (OCP)-mediated non-photochemical quenching (NPQ) of PBS fluorescence (Wilson et al. 2006). State transitions provide the balance of absorbed energy between the PSI and PSII depending on the redox state of electron carriers between photosystems (Bonaventura and Myers 1969; Fork and Satoh 1983). Light preferentially exciting PSI causes oxidation of the PQ pool and induces State 1, whereas the predominant excitation of PSII leads to PQ reduction and induces State 2 (Mullineaux and Allen 1990). Due to respiratory activity, dark-acclimated

cyanobacteria are usually in State 2, which is characterized by an increase of the effective antenna size of PSI, and they go to State 1 when illuminated with moderate white light to activate light absorption by PSII and compensate strong oxidation potential of PSI (Mullineaux and Allen 1990). In *Synechocystis,* the lack of ApcD and ApcF inhibits state transitions. The lack of ApcF also decreases energy transfer to both photosystems (Calzadilla et al. 2019).

State transitions can be visualized by fluorescence measurements. When the PBS or the Chl are excited, State 2 is characterized by a low PSII/PSI fluorescence ratio in the 77 K spectra, whereas a high PSII/PSI fluorescence ratio is typical for State 1. During the period of photosynthetic induction upon illumination of dark-acclimated *Synechocystis* cells, State 2 – State 1 transition is reflected in the chlorophyll a (Chl a) fluorescence kinetics. The chlorophyll fluorescence induction curve has been labeled OJIPS(M)T, where OJIP represents the fast (< 1 s) phases reflecting sequential reduction of PSII quinone acceptors Q_A, Q_B, and plastoquinone (PQ). The PS(M)T transition designates the slower (up to 10 min) phases of fluorescence induction (Govindjee 1995). The I-P rise, which reflects the filling up of the PQ pool, is followed by the S minimum. In PBS-containing cyanobacteria, the minimum S often precedes a subsequent slow (tens of seconds) S–M rise to the M level (Stirbet et al. 2019). This rise reflects State 2 – State 1 transition (Kaňa et al. 2012; Papageorgiou et al. 2007).

The mechanism of state transition in cyanobacteria is still unknown. Several mechanisms, including reversible PBS movement from PSII to PSI, direct transfer of the excitation energy from PSII to PSI core chlorophyll (spillover), partial PBS detachment from photosystems, reversible PSII quenching, and combinations of them, were proposed (Calzadilla and Kirilovsky 2020). According to recent studies, a strong decrease of PSII fluorescence in State 2 was mainly attributed to a reversible direct quenching of the PSII core, which was different from OCP-dependent NPQ, taking place at the PBSs level (Bhatti et al. 2020; Chukhutsina et al. 2015; Ranjbar Choubeh et al. 2018). The increase in fluorescence in State 1 was attributed to the functional detachment of PBSs from the photosystems (Chukhutsina et al. 2015; Kaňa et al. 2012).

Non-photochemical quenching in cyanobacteria is implemented with the participation of a carotenoid molecule as part of the 35 kDa water-soluble orange carotenoid protein (Gwizdala et al. 2011; Kirilovsky and Kerfeld 2012), which carries out directed delivery of the quencher, carotenoid, to the light-excited PBS. This process is induced as a result of photoexcitation of the carotenoid in the protein matrix (Yaroshevich et al. 2021), which leads to changes in the OCP structure and the formation of a red signaling state (Leverenz et al. 2015) responsible for thermal energy dissipation. This state is characterized by high conformational mobility of the OCP structure (Golub et al. 2019b) and a tendency to dimerization due to protein–protein contacts between C-domains (Golub et al. 2019a). Recent structural studies show that this dimeric form is able to interact with the phycobilisome in a way that two dimers of the OCP bind to the core of the phycobilisome (Domínguez-Martín et al. 2022). The energetic coupling between carotenoid and antennal pigments leads to a significant reduction in the lifetime of their excited states and decreases the probability of energy transfer to chlorophyll of photosystems and, consequently, photosynthetic activity under increased insolation (Protasova et al. 2021).

It is generally assumed that the state transitions in cyanobacteria occur only when dark-acclimated cells are exposed to low, non-saturating light intensities (Mullineaux and Emlyn-Jones 2004), whereas at high light intensity, the photoprotective effects are mainly associated with the OCP-dependent fluorescence quenching. However, in the dark-acclimated *Synechocystis* mutants, unable to form the flavoprotein Flv1/Flv3 heterodimer, we observed the State 2 – State 1 transition even when the cells were illuminated with very strong light (more than 2000 μmol m^{-2} s^{-1}) (Elanskaya et al. 2021). The deficiency in Flv1/Flv3 heterodimer in *Synechocystis* mutants led to changes in photoinduction of electron transfer upon dark–light transition, which affected the kinetics of redox transformations of P700 and induction of chlorophyll (Chl) fluorescence. Unlike the dark-acclimated wild type (WT) *Synechocystis* cells, in which LET was activated after the first 500 ms of illumination, the PSI-dependent CET lasted for the first 5–8 s in the mutants (Bulychev et al. 2018). P700 oxidation in the mutants was accompanied by a transient re-reduction stage, which coincided in time with S-M fluorescence rise, reflecting State 2 – State 1 transition (Kaňa et al. 2012). The lack of state transitions in *Synechocystis* WT cells illuminated with high light makes Flv1/Flv3-deficient mutants an attractive model for studying the relationships between OCP-dependent fluorescence quenching and state transitions. To this end, we introduced the mutant *apcD* and/or *ocp* genes into the *Synechocystis* strain deficient in Flv1 protein and studied the dynamics of light-induced changes in the constructed mutants upon dark–light transition.

Materials and methods

Strains and culture conditions

Synechocystis PCC 6803 WT cells were grown photoautotrophically for 4–5 days in a liquid BG-11 medium containing double the amount of sodium nitrate, with ambient CO_2 at 30 °C under continuous white light irradiance of 40 μmol m^{-2} s^{-1}. The samples were continuously stirred. The mutants were grown under the same conditions as

WT but the medium was supplemented with appropriate antibiotics: kanamycin (Km) at a final concentration of 100 μg mL^{-1}, chloramphenicol (Cm) and spectinomycin (Sp) at 20 μg mL^{-1} each. The *Synechocystis* sp. PCC 6803 glucose-tolerant strain used as the WT and the mutant strain Δ*flv1* (Cm^R) lacking flavodiiron protein Flv3 (Helman et al. 2003) were kindly provided by E.-M. Aro (University of Turku, Finland). Recombinant plasmids carrying the deletion variants of *apcD (sll0928*) and *ocp* (*slr1963*) genes were constructed by replacing parts of *apcD* and *ocp* genes with Km^R (Kuzminov et al. 2014) and Sp^R (Protasova et al. 2021) cassettes, correspondingly. The recombinant plasmids were used to transform by double recombination the Δ*flv1* mutant. The double Δ*flv1*/Δ*apcD* (Cm^R/Km^R) and Δ*flv1*/Δ*ocp* (Cm^R/Sp^R) clones were selected and segregated. The triple Δ*flv1*/Δ*apcD*/Δ*ocp* mutant was constructed by transformation of Δ*flv1*/ strain with a plasmid carrying the deletion variant of *ocp* gene with selection of Cm^R/Km^R/Sp^R clones. Segregation was confirmed by PCR. Prior to measurements of Chl fluorescence, P700 redox transients, and dynamic changes of LET and CET, the cells were harvested and resuspended in the same BG-11 medium at chlorophyll concentration of 10 μg mL^{-1}.

Induction curves of chlorophyll fluorescence

Changes in Chl fluorescence were measured with a Plant Efficiency Analyzer (PEA, Hansatech Instruments, UK). Fluorescence was induced by red light at photon flux densities of 200 and 2000 μmol quanta m^{-2} s^{-1} (excitation band 580–700 nm, maximum emission at 650 nm). Samples (300 μL cell suspension) were kept for 5 min in darkness prior to measurements. The illumination period (100 s) was sufficiently long to observe a slow S-M stage of the induction curve or the lack of this stage in some mutants.

Absorbance changes at 810 nm

Redox transients of P700 chlorophyll in PSI reaction centers were measured from changes in absorbance difference at 810 and 870 nm ($\Delta A_{810\text{-}870}$) as described in (Elanskaya et al. 2021). The measuring system consisted of a PAM-101 control unit (100 kHz modulation frequency) and ED-P700DW dual-wavelength emitter–detector unit (Walz, Germany). A multi-branch fiber-optic cable 101-F5 (Walz) was used to guide modulated measuring beam and actinic light toward the sample and to direct transmitted infrared light to the detector. The sample (200 μL) was placed between a mirror support and the end of the fiber-optic cable and kept in darkness for 5 min before measurements. Considering that state transitions in WT cyanobacteria are best pronounced at dim light and are absent at high intensity light, we employed low (200 μmol quanta m^{-2} s^{-1}) and high (2000 μmol quanta m^{-2} s^{-1}) photon flux densities of actinic light to verify the occurrence of this established trait for WT *Synechocystis* PCC 6803 cells.

The samples intended for $\Delta A_{810\text{-}870}$ measurements were illuminated with neutral white light (WL) of a Luxeon LXK2-PWN2-S00 light-emitting diode (100 lm, 700 mA, 4100 K; Lumileds, USA). The far-red (FR) light was obtained from LED with the maximum emission at 740 nm and a half bandwidth of 14 nm. Photon flux densities provided by LED sources of WL and FR light were 2000 and 400 μmol m^{-2} s^{-1}, respectively. A LED with the peak emission at 590 nm (orange light) was used for predominant excitation of phycobilisomes. The incident photon flux density was 160 μmol m^{-2} s^{-1}. The acquisition of $\Delta A_{810\text{–}870}$ signals and the timing control of light pulses from LED sources were carried out by means of a PCI-6024E analog–digital converter (National Instruments, USA) and WinWCP software (Strathclyde Electrophysiology Software).

Low-temperature fluorescence emission spectra

The low-temperature (77 K) fluorescence emission spectra were recorded with a Fluorolog-3 instrument (Horiba Jobin Ivon, Japan-France) equipped with a home-made cryostat. The samples were placed into glass capillaries having 2 mm internal diameter and immersed into a Dewar quartz vessel filled with liquid nitrogen. The spectra were recorded upon the excitation at 580 nm in the band of phycobilin absorption. The bandwidth slits were 4 nm for the excitation light and 2 nm for the emission light. The fluorescence spectra were normalized to the peak at 723 nm. The following protocol was used to detect state transitions. State 2 was induced by dark incubation of cyanobacteria for 30 min. In order to achieve State 1, the cells were treated with 50 μM DCMU [3-(3,4-dichlorophenyl)-1,1-dimethylurea] in darkness, placed into a glass capillary, and exposed for 2 min to white light at three light intensities (2860, 130, and 43 μmol quanta m^{-2} s^{-1}). Thereafter, the sample was quickly immersed into liquid nitrogen in order to avoid the backward transition. The recorded low-temperature spectra were averaged based on three measurements. The occurrence of State 2–State 1 transitions was inferred from the ratio of PSII fluorescence intensities at 684 and 692 nm and the intensity of PSI fluorescence band at 723 nm; the average values were calculated. The relative change of PSII/PSI fluorescence ratio in the illuminated sample (in State 1) with respect to the dark sample (in State 2) served as an indicator of state transitions.

Measurements of fluorescence quenching induced by OCP

Fluorescence changes reflecting the OCP-induced quenching of WT *Synechocystis* and its mutants were recorded by

time- and wavelength-correlated single photon counting setup based on HMP-100-07C detector and SPC-150 module (Becker &Hickl, Germany). Fluorescence excitation was performed by second harmonics of optical parametric oscillator TOPOL (Avesta Project LTD., Moscow, Russia) pumped by Yb femtosecond laser TEMA-150, (Avesta Project LTD., Moscow, Russia), driven at 80 MHz repetition rate, delivering 150 fs pulses to the sample at 620 nm. The excitation laser power was set to 0.5 mW. Fluorescence detection was performed in the 670-nm region using a ML-44 monochromator (Solar, Belarus). The TCSPC hardware was operated in the FIFO mode, recording a time-course of fluorescence intensity together with picosecond fluorescence decay. Temperature of the sample was controlled by a Qpod 2e (Quantum Northwest, USA) cuvette holder. Photoactivation of OCP was triggered by 180 µmol m^{-2} s^{-1} 445 nm blue LED (Thorlabs, USA) driven by a LED driver (DC2200, Torlabs, USA). All experiments were conducted at 25 C.

Modulation of linear and cyclic electron transport pathways in the induction period

The dynamic changes of linear electron transport (LET) and cyclic electron transport (CET) in the WT and mutants were assessed by applying a tandem combination of white light (WL, 2000 µmol m^{-2} s^{-1}) and far-red light (FR, 400 µmol m^{-2} s^{-1}) pulses (Bulychev et al. 2018). The duration of WL pulse increased sequentially from 0 to 10 s with an increment of 500 ms, while the separating interval between WL and a 1-s FR pulses remained constant (100 ms). The tandem pulses were applied in a sequential pattern with the separation time of 30 s. The analyzed parameters were the exponential time and the amplitude of exponential $P700^+$ dark reduction after the end of FR pulse. In the other modification of the experimental protocol, the duration of the WL pulse increased sequentially from 0 to 700 ms with an increment of 50 ms, while the parameters of FR pulses remained unchanged.

Figures display the results of representative experiments performed in at least four replicates with various cultures. Measurements on samples from individual cultures were performed in duplicates, with 5–10 assays per sample. The WT and mutants treated with inhibitors (15 µM DCMU, 100 µM DBMIB, 300 µM methyl viologen) were kept for 10 min in the dark before measurement. We used methyl viologen obtained from Acros Organics (Belgium), DCMU from Serva, and DBMIB from Sigma.

Results

Chl fluorescence induction and P700 redox changes in the mutants deficient in ApcD protein

Low light measurements

The delayed rise of chlorophyll (Chl) fluorescence (S–M stage in the fluorescence induction curve) has been recognized as a suitable indicator of State 2 – State 1 transition in cyanobacteria (Kaňa et al. 2012). As can be seen in Figs. 1A and B, the S-M stage of the induction curve was well pronounced in WT *Synechocystis* at low light intensity but was missing in the Δ*apcD* mutant deficient in PBS core component ApcD (α-subunit of allophycocyanin B). This result is in line with previous findings that the lack of ApcD leads to inhibition of state transitions (Ashby and Mullineaux 1999; Calzadilla et al. 2019).

By contrast to Δ*apcD* mutation, the deficiency in flavodiiron proteins Flv1/Flv3 was shown to promote State 2 – State 1 transition and prolong cyclic electron flow at early stages of photosynthetic induction, when electron acceptors of linear pathway behind PSI are not yet available after dark acclimation (Bulychev et al. 2018; Elanskaya et al. 2021). These features can be seen in Fig. 1C, where the S–M stage is well pronounced in Δ*flv1* mutant. The prolonged operation of CET was accompanied by long-lasting reduction of electron transport chain. The transient reduced state of P700 after its primary oxidation lasted for several seconds, and the duration of PQ/Q_B reduced state (fluorescence at P level) was also extended. The secondary oxidation of P700 (B–C) started in 5–6 s from the beginning of cell illumination; then the oxidation was interrupted approximately at the 10th second and was replaced by a transient reduction of $P700^+$ (C–D decline). The eventual large oxidation of P700 in the time range of tens of seconds continued at the same rate as at the initial stage, which was obviously determined by the rate of linear electron flow after the activation of FNR and Calvin cycle. The maximum oxidation level of P700 was reached after about 1 min of illumination and coincided with the maximum M on the fluorescence induction curves (Fig. 1C). Thus, the S-M rise of Chl fluorescence reflecting the State 2 – State 1 transition corresponds to different events in PSI; transitory reduction of $P700^+$ and subsequent oxidation of P700 to a stationary level.

Parallel measurements of Chl fluorescence and P700 redox transients with the double mutant lacking both ApcD and Flv1 proteins yielded unexpected results (Fig. 1D). In this mutant, the lack of ApcD did not prevent completely the S-M fluorescence rise indicative of State 2 – State 1 transition. The M peak of fluorescence was still higher

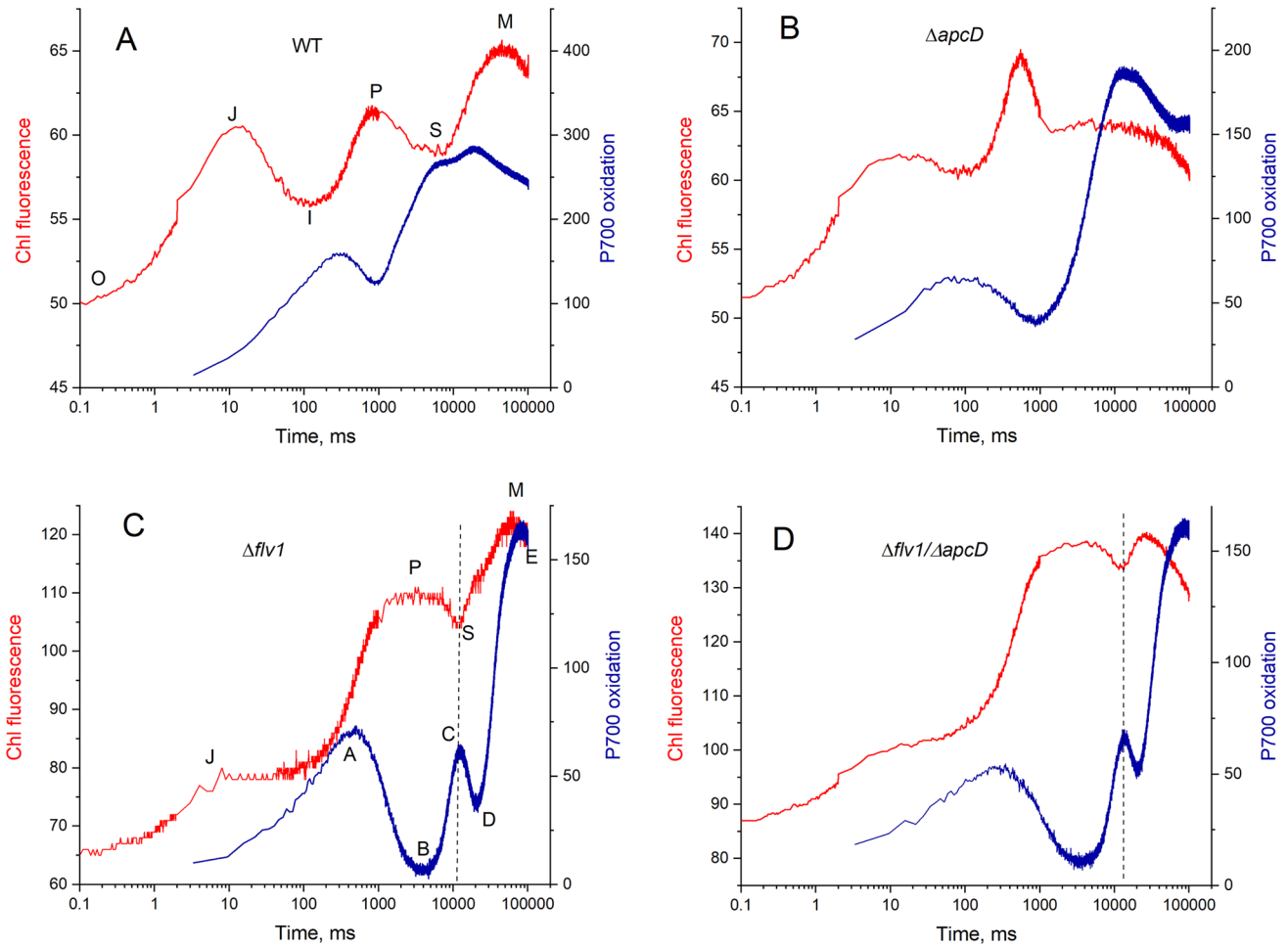

Fig. 1 Light-induced changes in chlorophyll fluorescence and P700 oxidoreduction state in WT *Synechocystis* and in the mutants deficient in Flv1, ApcD, and Flv1/ApcD exposed to low intensity light (200 µmol m^{-2} s^{-1}). **A** WT; **B** Δ*apcD* mutant; **C** Δ*flv1* mutant; **D** Δ*flv1*/Δ*apcD* mutant

than the peak P, and the S–M rise was accompanied by the transient reduction of $P700^+$. However, the M/P peak ratio of the Δ*flv1*/Δ*apcD* double mutant was markedly lower compared to Δ*flv1* mutant, indicating a partial suppression of the State 2 – State 1 transition in the absence of ApcD.

High light measurements

State transitions are commonly regarded as an adjustment mobilized upon low light treatments, while they are less pronounced or absent under exposure of cyanobacteria to strong light (Mullineaux and Emlyn-Jones 2004). The exposure of WT *Synechocystis* to high light (Fig. 2A) did not induce S-M rise in Chl fluorescence indicating the lack of State 2 – State 1 transition. When the mutant deficient in ApcD was exposed to high intensity light, the fluorescence decreased monotonically after the peak P, and the S-M stage was absent (Fig. 2B). Unlike WT, the lack of Flv1 protein promoted the development of S-M fluorescence rise also at high intensity light (Fig. 2C). It is seen that the peak M was the dominant one in the fluorescence induction curve recorded at high irradiance. The exposure to high light of the double mutant deficient in ApcD and Flv1 was accompanied by the appearance of S-M rise and the respective stage of $P700^+$ reduction (Fig. 2D); however, the amplitude of peak M in comparison to P maximum was largely decreased. The results in Fig. 1 and Fig. 2 suggest that the lack of Flv1 protein promotes the occurrence of State 2 – State 1 transition not only under dim illumination but also at high irradiance, and the absence of ApcD protein did not cause complete suppression of the S-M rise in Flv1-less mutant.

77 K emission spectra

Low-temperature fluorescence spectra represent a reliable method for the detection of state transitions in photosynthetic preparations. We employed this technique to compare fluorescence emission spectra for Δ*flv1* mutant and the

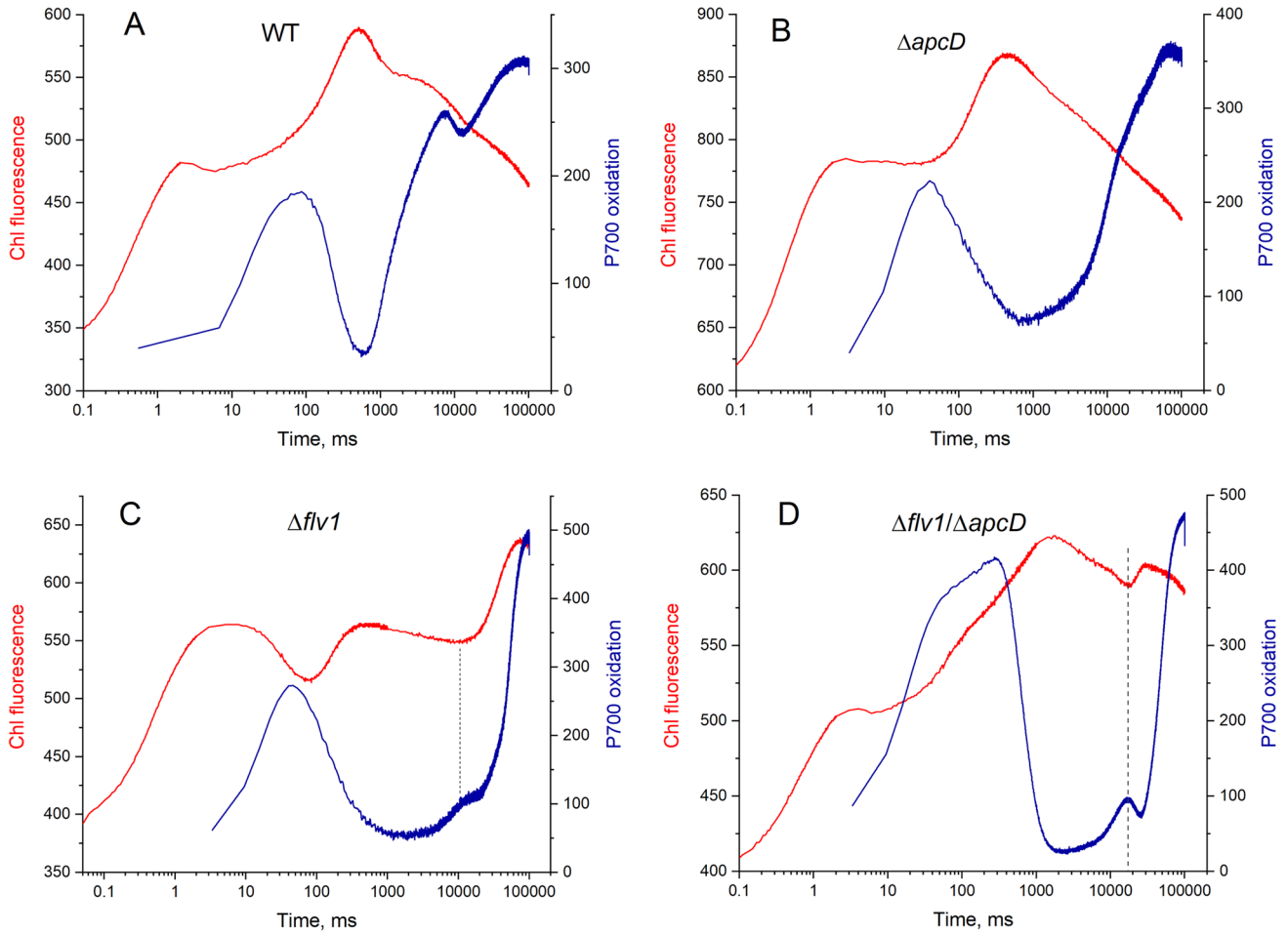

Fig. 2 Light-induced changes in Chl fluorescence (red) and P700 oxidoreduction state (blue) in WT *Synechocystis* and in the Flv1, ApcD, and Flv1/ApcD deficient mutants exposed to high intensity light (2000 µmol m^{-2} s^{-1}). **A** WT; **B** Δ*apcD* mutant; **C** Δ*flv1* mutant; **D** Δ*flv1*/Δ*apcD* mutant

mutant lacking both Flv1 and ApcD proteins (Fig. 3). The constant level of fluorescence emission of PSI during State 1/State 2 transitions in *Synechocystis* (Bolychevtseva et al. 2021; Choubeh et al. 2018; Stadnichuk et al. 2009) allows evaluating the state transitions as a change in the ratio of PSII/PSI fluorescence emissions. As can be seen in Fig. 3A, the fluorescence band at 684 nm normalized to the peak at 723 nm became higher in the Δ*flv1* mutant after exposure to strong white light, which indicates the occurrence of State 2 – State 1 transition upon illumination of this mutant. Upon excitation at 580 nm of phycocyanin, which is the major phycobiliprotein in PBSs of *Synechocystis*, there was a large increase in shortwave fluorescence (at 650–665 nm) in Fig. 3A, which suggests that a part of PBS was functionally dissociated in strong light from the reaction centers and had its own enhanced emission.

In the Δ*flv1*/Δ*apcD* mutant (Fig. 3B), the ratio of peak emissions at 684 and 723 nm was notably higher than in Δ*flv1* strain, indicating that a larger portion of energy absorbed by PBS was directed to PSII and that the Δ*flv1*/Δ*apcD* as well as Δ*apcD* cells are fixed in State 1, as was observed before in this mutant (Ashby and Mullineaux 1999; Bhatti et al. 2020). An important feature is that the fluorescence band at 684 nm in the Δ*flv1*/Δ*apcD* mutant only slightly increased in illuminated compared to dark-acclimated sample (Fig. 3B). This observation indicates a significant suppression of State 2 – State 1 transition in the Δ*flv1*/Δ*apcD* mutant. The dissociation or PBS from the core antenna under strong light was less conspicuous in Δ*flv1*/Δ*apcD* than in Δ*flv1* mutant.

Chl fluorescence induction and P700 redox changes in the mutants deficient in OCP protein

Measurements at low and high light conditions

Non-photochemical fluorescence quenching involving orange carotenoid protein (OCP) is the main defense

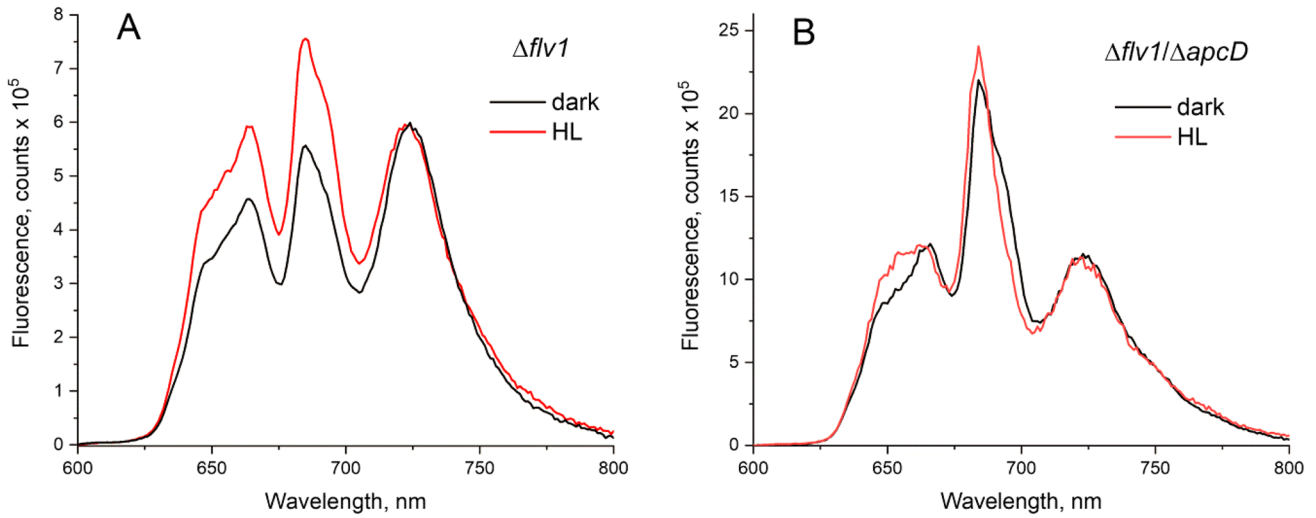

Fig. 3 Fluorescence emission spectra at 77 K of **A** *Synechocystis* Δ*flv1* mutant and **B** Δ*flv1*/Δ*apcD* mutant in dark-acclimated state (black curve) and after 2-min illumination of samples at room temperature with high intensity white light (HL, 2860 µmol m^{-2} s^{-1}) in the presence of 50 µM DCMU (red curve). The excitation wavelength (580 nm) was absorbed by phycobilisomes. Spectra were normalized to the peak at 723 nm

mechanism against strong illumination in *Synechocystis* (Gwizdala et al. 2011; Kirilovsky and Kerfeld 2012). We examined whether the deficiency of OCP modifies the fluorescence induction curves and how the absence of both OCP and Flv1 affects the capacity of cells to undergo state transitions. Figure 4 shows fluorescence induction curves and P700 redox transients in Δ*ocp* and Δ*flv1*/Δ*ocp* mutants exposed to low and high intensity light.

As in WT *Synechocystis*, the S–M stage of the induction curve was well pronounced in Δ*ocp* mutant at low intensity light (Fig. 4A) and absent at high light (Fig. 4C). In Δ*flv1*/Δ*ocp* mutant the transient reduction of intersystem electron carriers (Q_B, PQ) and P700 was prolonged for several seconds, during which CET presumably dominated (Bulychev et al. 2018; Elanskaya et al. 2021) (Fig. 4B, D). The S–M rise of Chl fluorescence was well pronounced at low light intensity in the double mutant, and the peak M was markedly higher than the peak P. Similar experiments carried out at high intensity light (2000 µmol m^{-2} s^{-1}) revealed the pronounced development of S–M fluorescence induction stage in Δ*flv1*/Δ*ocp* mutant (Fig. 4D). Hence, the lack of OCP had no significant influence on the occurrence of State 2 – State 1 transition in Flv1 deficient strain. It should be noted that the onset of S-M stage in the induction curve of Chl fluorescence was concurrent with the transient P700 reduction, in consistency with data shown in Figs. 1C, D.

77 K emission spectra

Analysis of low-temperature fluorescence spectra in Δ*ocp* and Δ*flv1*/Δ*ocp* mutants (Fig. 5) revealed that, as well as in the case of WT cells, the exposure of Δ*ocp* mutant to high light irradiance (2860 µmol m^{-2} s^{-1}) produced no State 2 – State 1 transition: the proportions of fluorescence peaks at 684–692 and 723 nm remained unchanged (Fig. 5A). Only at the low irradiance tested (43 µmol m^{-2} s^{-1}), the fluorescence of PSII normalized to the emission of PSI became higher than in the dark-acclimated cells. In the Δ*flv1*/Δ*ocp* mutant, a large increase in PSII fluorescence compared to PSI emission at 723 nm was observed at low and high light intensities. These spectral changes are consistent with the supposed occurrence of State 2 – State 1 transition in the mutant lacking both OCP and Flv1. Illumination of the Δ*flv1*/Δ*ocp* mutant at all irradiances tested also led to the increase in emission of PBS pigments at 650–665 nm, indicating the functional dissociation of PBS from the core antenna (Fig. 5B). A higher ratio of the PSII/PSI fluorescence emission at low light in comparison to high light in the Δ*flv1*/Δ*ocp* mutant (deficient in OCP) shows that the decrease in the peak of fluorescence at high light is not associated with the OCR-dependent quenching of fluorescence.

Chl fluorescence induction and P700 redox changes in the triple mutant deficient in Flv1, ApcD, and OCP

Like the double mutant lacking Flv1 and ApcD, under strong illumination, the triple Δ*flv1*/Δ*apcD*/Δ*ocp* mutant exhibited only a slight increase in S-M stage in the fluorescence induction curve, which coincided in time with the intermediate reduction of $P700^+$ (Fig. 6A). The 77 K fluorescence spectra of the triple mutant under high light showed no significant differences from the corresponding spectra of the double

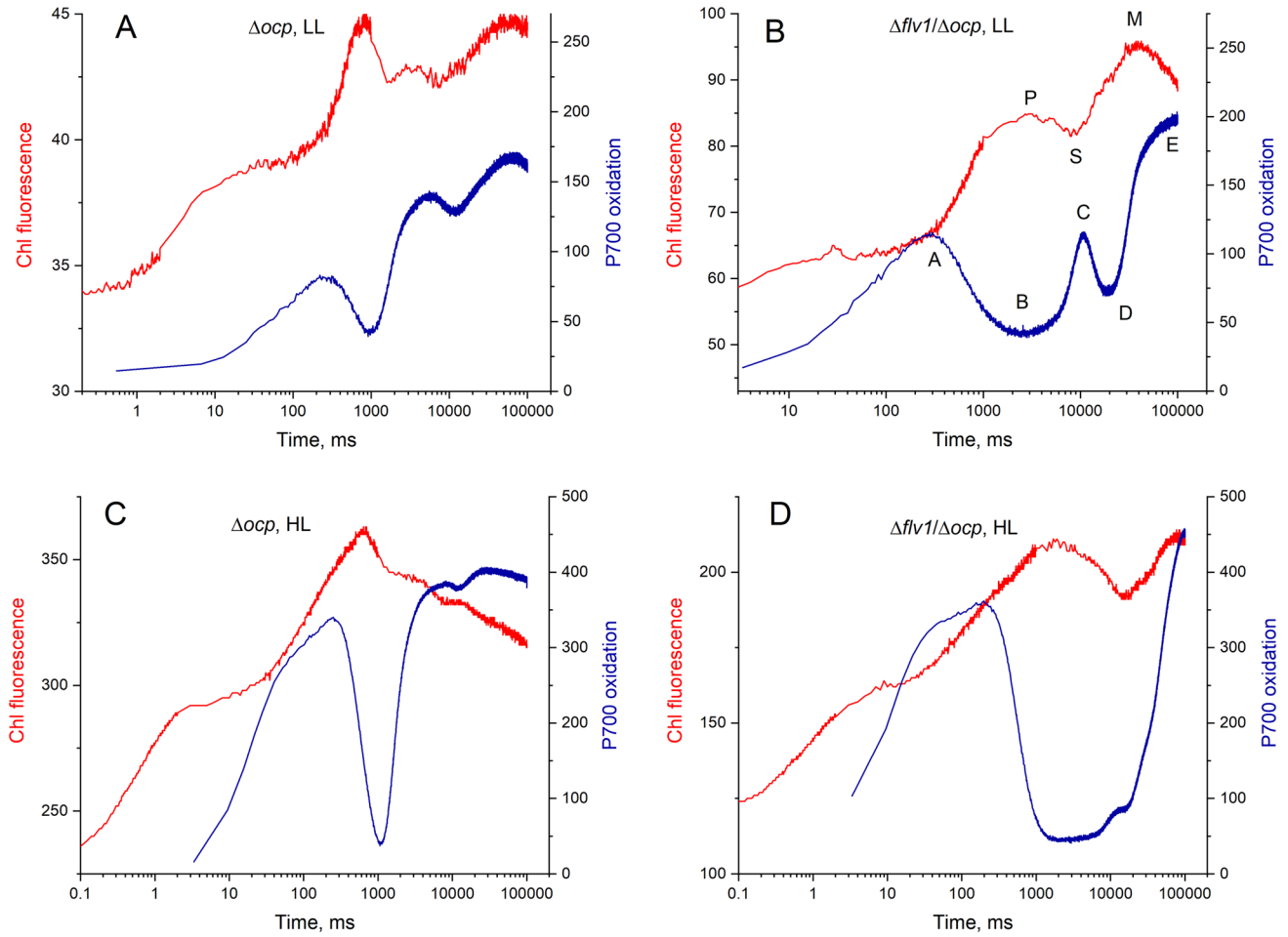

Fig. 4 Light-induced changes in chlorophyll fluorescence (red) and P700 oxidoreduction state (blue) in Δ*ocp* and Δ*flv1*/Δ*ocp* mutants of *Synechocystis*: **A** and **B** at low light intensity (LL, 200 µmol m^{-2} s^{-1}); **C** and **D** at high light intensity (HL, 2000 µmol m^{-2} s^{-1})

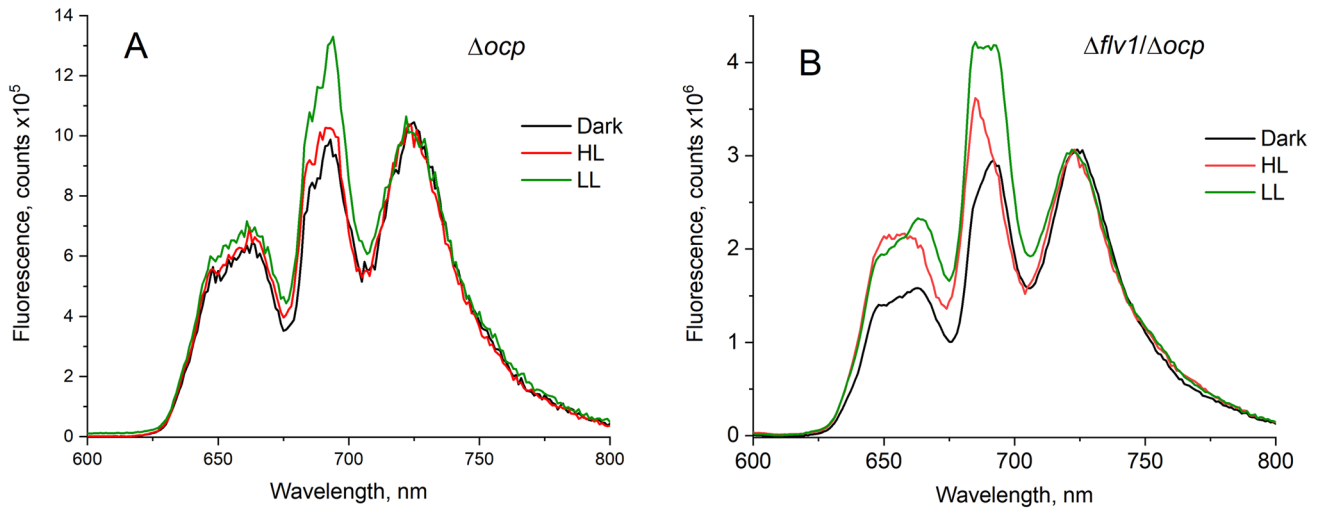

Fig. 5 Fluorescence emission spectra at 77 K of *Synechocystis* Δ*ocp* mutant (**A**) and Δ*flv1*/Δ*ocp* mutant (**B**) in dark-acclimated state (black curves) and after 2-min illumination of samples at room temperature with high intensity (2860 µmol m^{-2} s^{-1}, red curves) and low intensity (43 µmolm^{-2} s^{-1}, green curves) white light in the presence of 50 µM DCMU. The excitation wavelength 580 nm was absorbed by phycobilisomes. All spectra were normalized to the peak at 723 nm

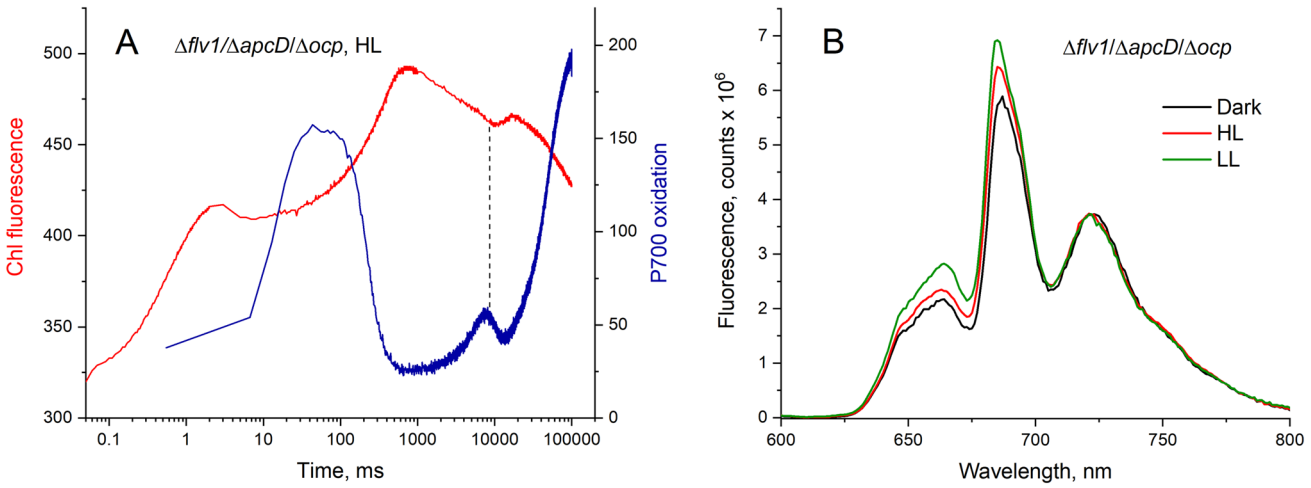

Fig. 6 (A) Light-induced changes in Chl fluorescence (red) and P700 oxidoreduction state (blue) of *Synechocystis* Δ*flv1*/Δ*apcD*/Δ*ocp* mutant. (B) fluorescence emission spectra at 77 K of Δ*flv1*/Δ*apcD*/Δ*ocp* mutant in dark-acclimated state (black curves) and after 2-min illumination of samples at room temperature with high intensity (2860 µmol m^{-2} s^{-1}, red curves), and low intensity (43 µmolm^{-2} s^{-1}, green curves) white light in the presence of 50 µM DCMU. The excitation wavelength at 580 nm was absorbed by phycobilisomes. All spectra were normalized to the peak at 723 nm

mutant Δ*flv1*/Δ*apcD*. (Fig. 6B). Thus, the deficiency in ApcD led to the inhibition of state transition regardless of OCP presence.

Energy transfer from PBS to PSI

It was shown that the absence of ApcD does not affect energy transfer to PSII and PSI in *Synechocystis* (Calzadilla et al. 2019). Nevertheless, the above data may indicate that PSI receives fewer excitations in the absence of Flv1. Therefore, we compared the wild-type *Synechocystis* with Δ*apcD,* Δ*flv1,* Δ*flv1*/Δ*apcD,* and Δ*flv1*/Δ*apcD*/Δ*ocp* mutants in their ability to oxidize P700 chlorophyll under the action of orange light absorbed by PBS (590 nm) in the presence of DCMU (15 µM), DBMIB (100 µM), and methyl viologen (300 µM) (Calzadilla et al. 2019). These chemicals ensured the inhibition of PSII-driven electron flow, the prevention of electron donation to $P700^+$ from the PQ pool, and the sufficiency of electron acceptors for PSI. Under these conditions, the rate of P700 photooxidation is thought to reflect the delivery of excitations from the antenna pigments, primarily phycobilins, to the PSI reaction centers.

The kinetics of P700 oxidation was measured under light pulses with intensities of 160 µmol quanta m^{-2} s^{-1}. The P700 redox changes were normalized to the amplitude of P700 photooxidation. As shown in Fig. 7, the photooxidation of P700 in the Δ*apcD* mutant was not retarded and developed approximately at the same rate as in the WT cells. Other

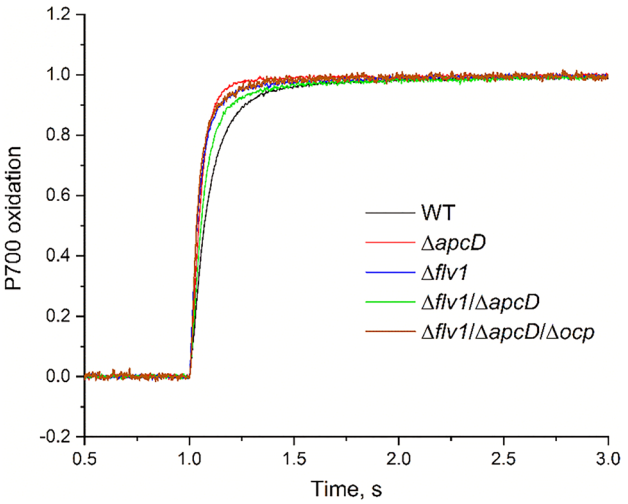

Fig. 7 Kinetics of P700 oxidation in WT *Synechocystis*, Δ*apcD*, Δ*flv1*, Δ*flv1*/Δ*apcD,* and Δ*flv1*/Δ*apcD*/Δ*ocp* mutants treated with 15 µM DCMU, 100 µM DBMIB, and 300 µM methyl viologen under exposure to orange light absorbed by phycobilisomes (590 nm) at 160 µmol quanta m^{-2} s^{-1}. Absorbance changes ($\Delta A_{810–870}$) were normalized to the amplitude of P700 photooxidation

mutants tested – Δ*flv1,* Δ*flv1*/Δ*apcD,* Δ*flv1*/Δ*apcD*/Δ*ocp* – displayed similar kinetics of P700 oxidation at low and elevated light intensities. Thus, the impairment of ApcD, Flv1, and OCP were not accompanied by the retarded delivery of excitations to PSI.

Rearrangement of cyclic and linear electron transport during photosynthetic induction in *Synechocystis*

Dynamic changes in cyclic and linear electron transport (CET and LET) at various stages of photosynthetic induction can be assessed by applying a tandem combination of white light pulse (WL, 2000 µmol m^{-2} s^{-1}, variable duration) and far red light (FR, 1100 µmol m^{-2} s^{-1}, 0.8 s) (Bulychev et al. 2018). After the first light pulse (WL), electrons delivered to the acceptor side of PSI distribute between linear and cyclic pathways having different influence on the redox state of the PQ pool. The second light pulse (intense FR light) oxidizes P700, while the subsequent $P700^+$ dark reduction proceeds faster or slower depending on the sufficiency or depletion of electrons in the PQ pool. Figure 8A shows the plots for the exponential time τ of $P700^+$ dark reduction after the FR pulse as a function of duration of the preceding WL pulse. The duration of the first WL pulse was 500 ms and durations of subsequent pulses were increased with an increment of 500 ms. The exposure of WT cells to WL pulses of extending durations was accompanied by the initial decrease in relaxation time τ (in the time range from 0 to 500 ms) and by the subsequent fast increase in this parameter. This temporal pattern suggests that CET is promoted at the initial stages of illumination until the LET is activated. Unlike WT strain, the mutants deficient in Flv1 exhibited a strong decrease in time τ upon the first pulse of WL illumination, and low τ values were maintained for 3–4 s. Then τ gradually increased with the prolongation of WL illumination. These data provide evidence for long-lasting operation of CET during the photosynthetic induction in the absence of Flv1 protein. Data on the change in the $P700^+$ signal

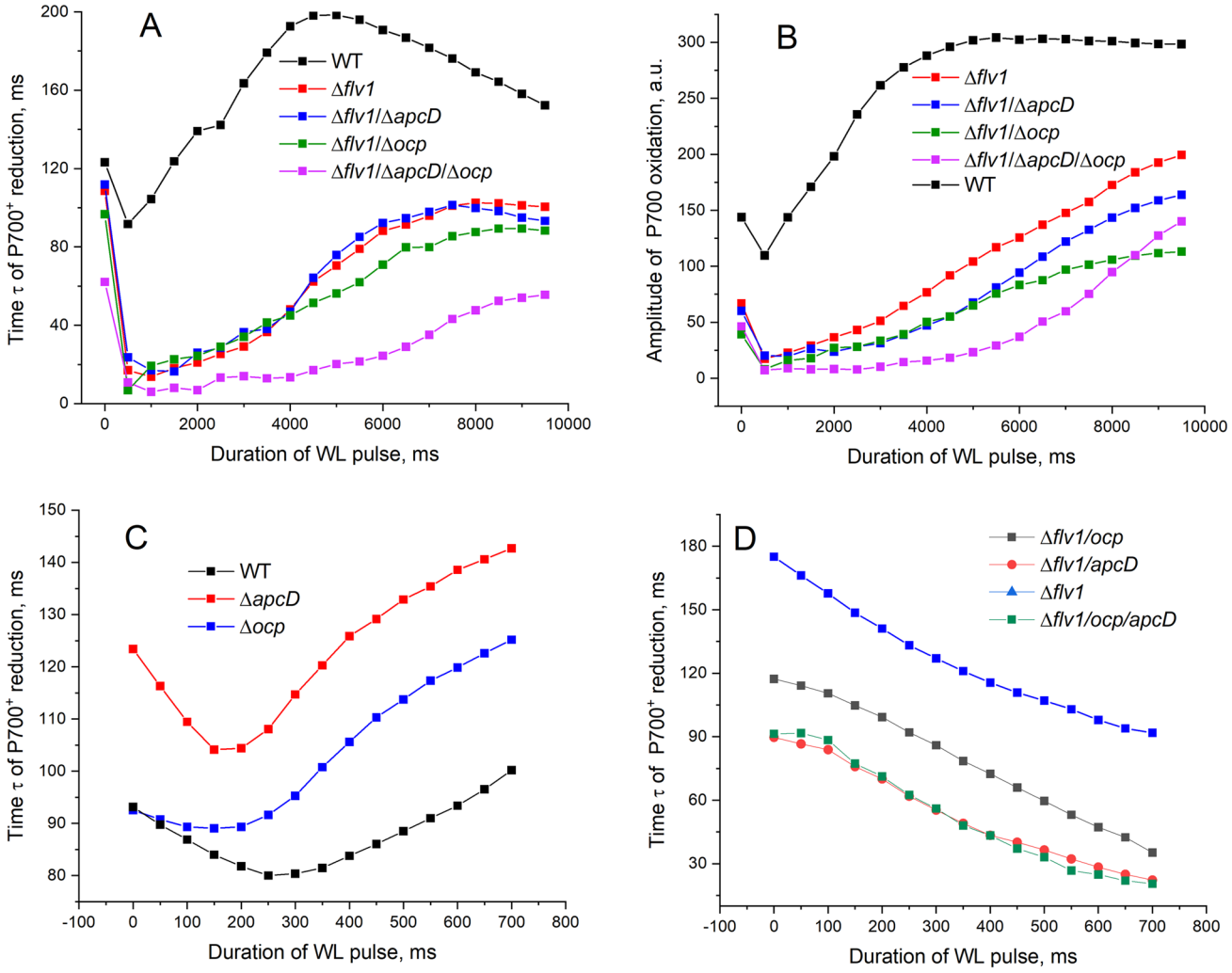

Fig. 8 **A**, **C**, **D** Time constants of $P700^+$ dark reduction after FRL-induced oxidation in wild-type, ApcD, Flv1, and Flv1/ApcD mutants preilluminated with WL pulses of various durations. Dark intervals from the end of WL to the onset of FRL were 100 ms; duration of FRL pulse, 0.8 s. **B** Amplitude of P700 oxidation at the end of FR pulse

amplitude, reflecting the level of P700 oxidation at the moment of termination of FR pulse (Fig. 8B), also show that in the WT, the stationary level of P700 oxidation is reached within 4–5 s of illumination with white light, while in mutants this takes more than 10 s. The effects of WL pre-exposure on the rate of P700 dark reduction (Fig. 8A) and the amplitude of FR-induced P700 oxidation (Fig. 8B) were particularly retarded in the triple mutant Δ*flv1*/Δ*apcD*/Δ*ocp*.

For a more complete analysis of τ changes in the first second after the start of WL illumination, we reduced the duration of the first WL pulse from 500 to 50 ms and extended the durations of subsequent pulses with an increment of 50 ms. In WT cells, Δ*apcD*, and Δ*ocp* mutants the decrease in τ in the first 200–300 ms of WL illumination was replaced by a rather rapid increase in τ, indicating activation of LET (Fig. 8C). In the Flv1-deficient mutants, only a decrease in τ was observed in the first second of WL illumination (Fig. 8D).

Blue-light induced fluorescence quenching in WT and mutants

In all samples containing OCP, we observed quenching of fluorescence with comparable efficiency, which starts approximately after 10 s of illumination and continues longer than 100 s (Fig. 9). On the contrary, in samples devoid of the gene encoding OCP, the fluorescence intensity was almost unchanged or slightly increased.

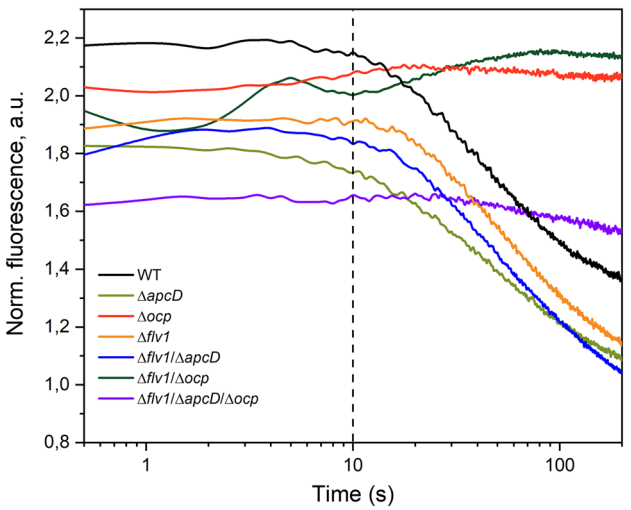

Fig. 9 Quenching of WT *Synechocystis* sp. PCC 6803 and its mutants fluorescence upon the exposure of cells to blue light (445 nm, 180 µmol photons m^{-2} s^{-1}) activating OCP. The time courses are normalized to fluorescence intensity values before the actinic LED is turned on. Fluorescence was recorded at 670 nm. The temperature of the cell suspension was stabilized at 25 °C

S–M fluorescence transient in Flv1 mutant treated with methyl viologen

In contrast to the Δ*flv1* mutants, which carry out the State 2 – State 1 transition at both low and high light intensities, in the WT the state transition occurred only when dark-acclimated cells were illuminated with low intensity light (Figs. 1, 2). Since the State 2 – State 1 transition upon illumination of cyanobacteria depends on the oxidation of PQ pool and, accordingly, P700, it can be expected that the addition of methyl viologen (MV), which accepts electrons from PSI, will restore the State 2 – State 1 transition under high light in WT cells.

Figure 10A shows light-induced changes in the redox state of P700 in dark-acclimated triple mutant Δ*flv1*/Δ*apcD*/Δ*ocp* in the absence and presence of 300 µM MV. Upon illumination with HL in the presence of this electron acceptor, the lag phase in P700 oxidation disappeared in the mutant and LET was rapidly activated, as in WT cells (Fig. 10A). In the induction curves of Chl fluorescence, the emission at peak P was largely suppressed, indicating the oxidation of ETC due to effective operation of MV as electron acceptor behind PSI (Fig. 10B). However, ETC oxidation did not lead to the appearance of S-M rise, possibly due to the absence of ApcD.

The induction curves of Chl fluorescence measured in the suspensions of WT and mutants (Fig. 11) show that the addition of 300 µM MV strongly suppressed the P peak achieved at approximately 1000 ms, indicating the transient oxidation of intersystem electron carriers (Q_B, PQH_2) similarly to observations with pea leaves infiltrated with 200 µM MV (Schansker et al. 2005). In WT cells illuminated with lowintensity light, MV addition did not inhibit the S-M rise (Fig. 11A) and it did not induce the S-M rise in the Δ*apcD* mutant in which the state transition is impaired (Fig. 11B).

Under high intensity light, the S–M rise indicating State 2 – State 1 transition in Δ*flv1* and Δ*flv1*/Δ*ocp* mutants, was observed both in the absence and in the presence of MV (Fig. 11D, E) and was strongly suppressed in WT (Fig. 11C) and Δ*flv1*/Δ*apcD* (Fig. 11F). Thus, the addition of MV, an artificial electron acceptor from PSI, does not affect the state transition in dark-acclimated cells under LL and HL illumination, and does not restore the ability to state transition in WT cells under HL.

Discussion

Upon dark–light transition of cyanobacteria, CO_2 fixation cannot start immediately after illumination and needs time for activation. During this period the following events must occur: (i) activation by light of a number of the Calvin cycle enzymes; (ii) accumulation of CO_2 in carboxysome in a

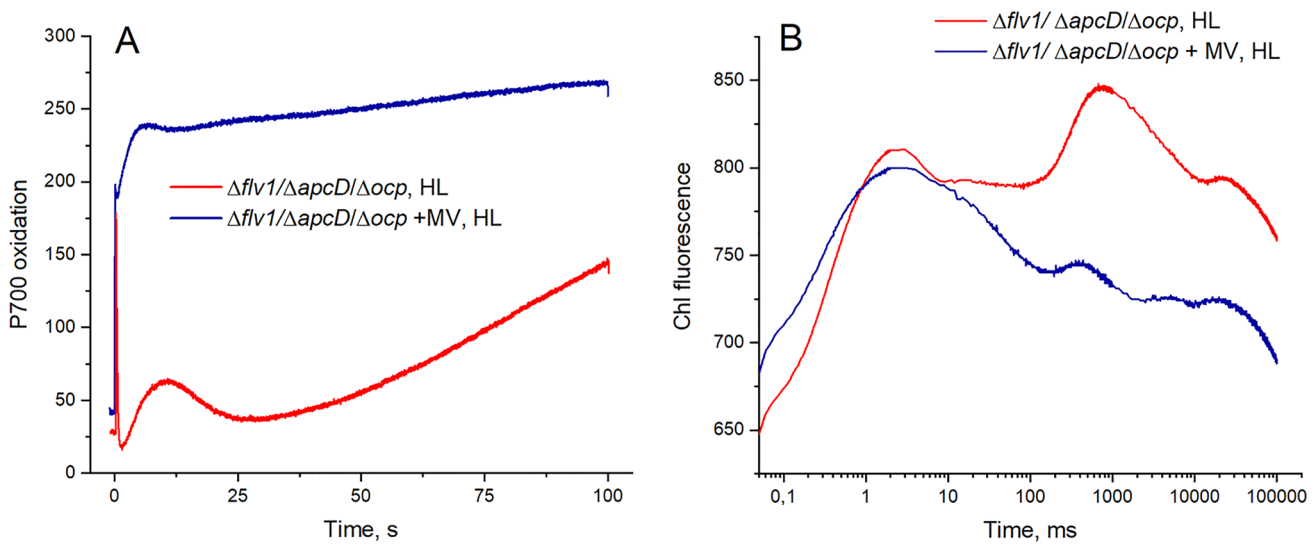

Fig. 10 Light-induced changes in **A** P700 redox state and **B** Chl fluorescence in Δ*flv1*/Δ*apcD*/Δ*ocp* mutant of *Synechocystis* at high light intensity (HL, 2000 µmol m^{-2} s^{-1}) in the absence (red curve) and in the presence (blue curve) of 300 µM methyl viologen (MV)

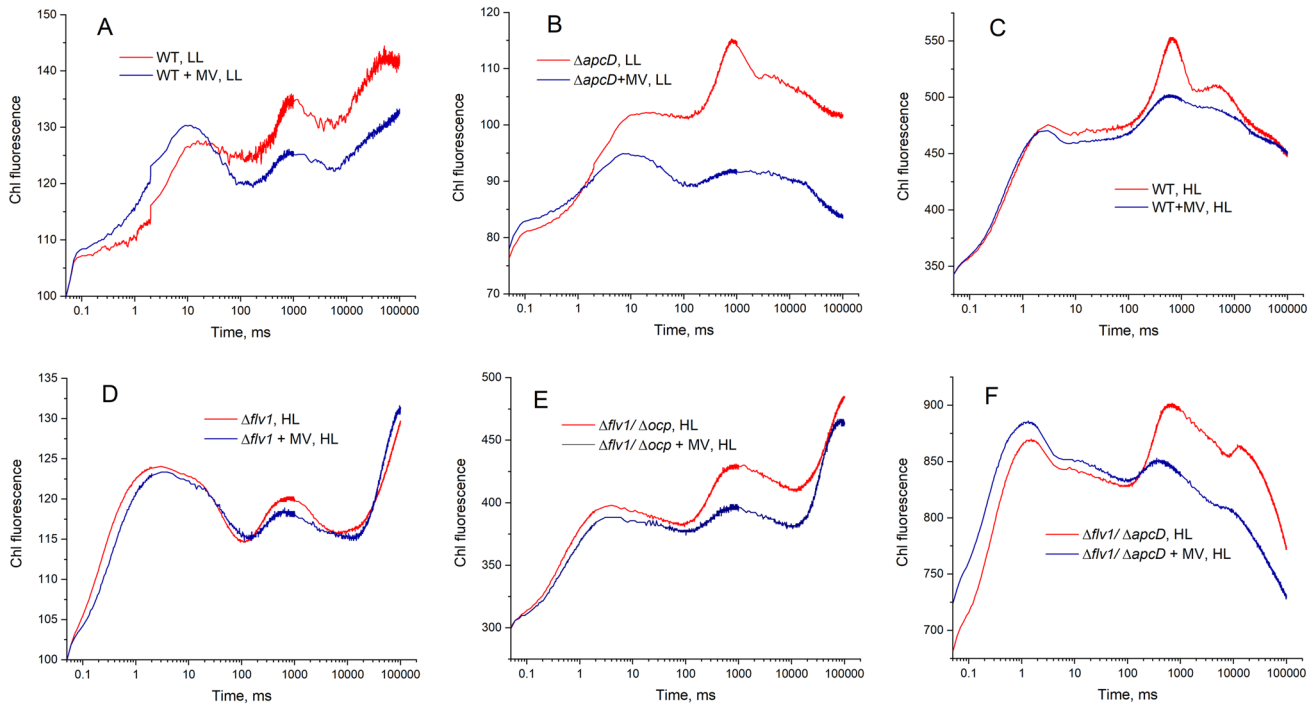

Fig. 11 The induction curves of Chl fluorescence in WT and mutants of *Synechocystis* at low (LL, 2000 µmol m^{-2} s^{-1}) and high light intensity (HL, 2000 µmol m^{-2} $s.^{-1}$) in the absence (red) and in the presence (blue) of 300 µM methyl viologen (MV). **A** WT, LL; **B** Δ*apcD*, LL; **C** WT, HL; **D** Δ*flv1*, HL; **E** Δ*flv1*/Δ*ocp*; HL; **F** Δ*flv1*/Δ*apcD*, HL.

concentration sufficient for the operation of RuBisCO; (iii) synthesis of NADPH and ATP as a result of the activation of FNR and the creation of a proton potential for the operation of ATPase. In cyanobacteria and chloroplasts, some Calvin cycle enzymes become inactivated in darkness and need light for their activation (Tamoi and Shigeoka 2015). The accumulation of CO_2 in the carboxysome takes about 20 s after illumination of dark-acclimated *Synechocystis* cells (Allahverdiyeva et al. 2011; Mustila et al. 2016) and during this time the genes encoding CO_2 and bicarbonate

uptake systems are upregulated (Saha et al. 2016). During the activation of FNR and the Calvin cycle enzymes, LET in *Synechocystis* is supported by the heterodimer of flavodiiron proteins Flv1/Flv3 accepting electrons from PSI (Allahverdiyeva et al. 2011; Helman et al. 2003).

During the period of the Calvin cycle activation in *Synechocystis* mutants unable to form the Flv1/Flv3 heterodimer (Bulychev et al. 2018; Elanskaya et al. 2021), as well as in angiosperms devoid of FDPs (Kramer et al. 2021; Noridomi et al. 2017), LET is replaced by CET, which allows the formation of the proton potential necessary for ATP synthesis. In the dark-acclimated WT, Δ*apcD* and Δ*ocp* mutants containing the Flv1/Flv3 heterodimer, illumination with strong white light led to a rapid (300–400 ms) change of CET to LET, and the maximum level of P700 oxidation tested by FR light was reached within 4–5 s (Fig. 8). On the contrary, in the Flv1-deficient strains, especially in the triple Δ*flv1*/Δ*apcD*/Δ*ocp* mutant, CET continued for a longer time (up to 5–6 s), and the stationary oxidation level of P700 was significantly lower than that of WT (Fig. 8B). In addition to the important role of the Flv1/Flv3 heterodimer in the photoinduction of electron transport through PSI, these data indicated possible participation of ApcD and OCP in this event.

Our analysis of fluorescence induction curves is based on a widely spread assumption that variable Chl fluorescence originates largely from PSII and that variable fluorescence of PSI is negligibly small. Schreiber and Klughammer in their recent paper (Schreiber and Klughammer 2021) argue that the contribution of PSI to the formation of peak P on the induction curve of Chl fluorescence is substantial, especially in cyanobacteria, which would necessitate the revision of the traditional views on the origin of I-P (I_2-P) transient. We focused mainly on the S-M transition that develops on a quite different time scale (100 s), at which the contribution of PSI to variable Chl fluorescence is not predicted.

In the WT *Synechocystis,* the S-M rise in chlorophyll fluorescence induction curves and an increase in the PSII/PSI ratio in the 77 K fluorescence spectra, indicating the transition of the photosynthetic apparatus from State 2 to State 1, were observed when the dark-acclimated cells were illuminated with relatively low intensity light. However, in the dark-acclimated *Synechocystis* mutants, unable to form the Flv1/Flv3 heterodimer, we observed the State 2–State 1 transition even when the cells were illuminated with strong light (Figs. 2C, 3A). This property of the mutant devoid of the Flv1/Flv3 heterodimer made it possible to use this mutant to study the relationship between state transitions and OCP-dependent fluorescence quenching.

For the state transitions, *Synechocystis* requires terminal phycobilisome acceptors ApcD and ApcF. While the lack of ApcF decreases energy transfer to both photosystems, deficiency in ApcD does not decrease energy transfer from PBS to any of the photosystems, but it inhibits state transitions (Ashby and Mullineaux 1999; Calzadilla et al. 2019). Mutants, deficient in the *apcD* gene encoding the α-subunit of the allophycocyanin B core subunit, have been shown to be impaired in state transitions and appear to be stuck in state 1 (Dong et al. 2009). In the present paper, we have shown that ApcD is important for the State 2 – State 1 transition in the Δ*flv1 Synechocystis* mutant, which is unable to form the Flv1/Flv3 heterodimer, even when illuminated with strong light. The introduction of the Δ*apcD* mutation into the Δ*flv1* strain significantly reduced the S-M rise in Chl fluorescence (Fig. 2C, D) and greatly reduced the level of the State 2 – State 1 transition in emission spectra of Chl fluorescence at 77 K compared to the original Δ*flv1* strain (Fig. 3). It should be noted that both low-temperature fluorescence emission spectra and induction curves of chlorophyll fluorescence were recorded upon the excitation at 580 nm in the band of phycobilin absorption. According to (McConnell et al. 2002), the excitation of PBSs is important for the manifestation of state transitions disorders in the Δ*apcD* mutant.

Since the OCP manifests itself only after its activation by blue or strong white light, the S-M rise in chlorophyll fluorescence induction curves obtained under orange-red light, does not reflect the effect of OCP on the photoinduction of electron transport. After the activation of OCP by blue light, quenching of fluorescence was observed in all strains carrying a wild copy of the *ocp* gene and was absent in Δ*ocp* mutants (Fig. 9). 77 K chlorophyll fluorescence spectra (Fig. 5B) indicate the State 2 – State 1 transition after illuminating the Δ*flv1*/Δ*ocp* mutant with strong white light. Thus, in the Flv1-deficient mutants, the absence of OCP does not affect the state transition when the cells were illuminated with strong white light, and the deficiency in ApcD did not impair OCP-dependent fluorescence quenching, as it was shown earlier for *Anabaena* PCC 7120 (Dong and Zhao 2008). A lower ratio of PSII/PSI fluorescence emission at high light compared to low light, observed in Δ*flv1*/Δ*ocp* mutant (Fig. 5B), indicates that the difference is not related to NPQ. Perhaps this is the result of irreversible inactivation (photoinhibition) of PSII under high intensity light (Aro et al. 1993; El Bissati et al. 2000).

Parallel measurements of light-induced changes in chlorophyll fluorescence, P700 redox transformations, fluorescence emission at 77 K, and OCP-dependent fluorescence quenching, revealed the time dependence of events occurring when dark-acclimated cells are illuminated. (i) the S-M rise in Chl fluorescence induction curves, reflecting State 2 – State 1 transition, started approximately 10 s after the beginning of cell illumination, and was observed in Δ*flv1* mutants both under weak and strong light, while in WT and Δ*ocp* mutant, the S-M stage was observed under weak light only (Figs. 1, 2, 4). (ii) In Δ*flv1* mutants, the start of

S-M rise always coincided in time with the beginning of the transient $P700^+$ re-reduction (C–D decline in Fig. 1C). (iii) The OCP-dependent fluorescence quenching appeared 10 s from the moment when the cells were exposed to high intensity light and was not registered until that time (Fig. 9). That is, in the interval between 10 and 20 s after the start of illumination, the photosynthetic apparatus of cyanobacteria undergoes a number of significant modifications that ensure its acclimation to the changed conditions.

Despite the fact that OCP-dependent fluorescence quenching, State 2 – State 1 transition, and the transient $P700^+$ re-reduction manifested themselves at the same time after the start of illumination, it is obvious that these processes occur independently of each other. OCP-dependent PBS fluorescence quenching occurred in Δ*apcD* mutants, deficient in state transitions, in the same way as in WT, and State 2 – State 1 transition was observed in Δ*flv1*/Δ*ocp* mutant incapable of NPQ. The transient $P700^+$ re-reduction was not associated with state transition or OCP-dependent fluorescence quenching, as it was observed in Δ*flv1*/Δ*apcD* and Δ*flv1*/Δ*ocp* mutants. Moreover, a weak transient $P700^+$ re-reduction could also be observed in strains containing Flv1/Flv3 heterodimer when there was no state transition, for example, under high light in WT (Fig. 2A) or in Δ*ocp* mutant (Fig. 4C). Apparently, all these processes are associated with a certain event in the photosynthetic apparatus, which occurs about 10 s after the illumination of dark-acclimated cells.

In Δ*flv* mutants the oxidation of P700 (B-C rise in $\Delta A_{810-870}$ curves) starts 5–6 s after exposure to light and coincides with fluorescence decline P–S in OJIPS(M) fluorescence kinetics. The P700 oxidation and the decrease in fluorescence, reflecting the re-oxidation of PQ pool, point to activation of FNR and Calvin cycle on the acceptor side of PSI (Mullineaux 2014; Tamoi et al. 2005). The transient $P700^+$ re-reduction may be a consequence of two (or one of two) events. Firstly, a decrease in the energy supply from phycobilisomes to P700 as a result of the PBS detachment from PSI (Chukhutsina et al. 2015). It has been shown that conventional PBS of *Synechococcus* sp. PCC 7002 containing CpcG1 linker protein (CpcG1-PBS) can transfer energy to PSI only if they contain ApcD protein (Dong et al. 2009). In Δ*apcD* mutants, another type of PBS, containing CpcG2 linker protein, efficiently transfered energy to PSI (Deng et al. 2012). In accordance with the data of (Calzadilla et al. 2019), our data (Fig. 7) also indicate, that the absence of ApcD does not affect energy transfer to PSI in *Synechocystis*. This may mean that PBS detachment from PSI in WT *Synechocystis* upon dark–light transition (Chukhutsina et al. 2015) applies only to CpcG1-PBS and does not occur in Δ*apcD* mutants. Secondly, PSII is partially inhibited in State 2 (Ranjbar Choubeh et al. 2018) and the transient re-reduction of $P700^+$ may be associated with a rapid reduction of the PQ pool as a result of PSII activation (Gerotto et al. 2016; Yamori 2016). It is important to note that the transient re-reduction of $P700^+$ starts with the beginning of the S–M rise in Chl fluorescence. In Δ*flv1*/Δ*apcD* mutants, the S–M rise is expressed only to a small extent and coincides in time with transient $P700^+$ re-reduction (Figs. 1, 2). This suggests that S-M rise in Δ*flv1* mutant includes two components: one of them really reflects the State 2 – State 1 transition, which is inhibited in the Δ*flv1*/Δ*apcD* mutant, and the second is ApcD-independent component, the starting point and duration of which coincide in time with the transient $P700^+$ re-reduction.

The redox state of the PQ pool is a key regulator of state transitions in cyanobacteria and chloroplasts. State 1 is established at highly oxidized PQ, whereas moderate reduction of the PQ pool induced the transition to State 2 (Calzadilla and Kirilovsky 2020; Minagawa 2011; Mullineaux and Emlyn-Jones 2004). In the dark, the PQ pool is partially reduced by the respiratory dehydrogenases, and the photosynthetic apparatus in cyanobacteria is in State 2. Under illumination with white light, which includes wavelengths specifically exciting both the PSII and PSI, redox state of the PQ pool depends on the ratio of electron transfer rates of the two photosystems, as preferential excitation of PSII or PSI causes reduction or oxidation of the PQ pool, respectively. Illumination with low or moderate white light slightly favoring PSI causes oxidation of the pool and induces the transition of the photosynthetic apparatus from State 2 to State 1 (Mattila et al. 2020). Strong light, in turn, reduces the PQ pool because the maximum rate of PQH_2 oxidation by Cyt b_6f is slower than the delivery of electrons to the PQ pool by PSII (Laisk et al. 2005). Under strong white light, the electron flow from PSII to PSI sharply increases, leading to the reduction of PQ pool. This could explain the absence of state transition in the WT under high light. In cyanobacteria the light-dependent State 2 – State 1 transition was enhanced by a PSI electron acceptor methyl viologen, which caused the PQ pool to become more oxidized in the light (Mullineaux and Allen 1990). We used methyl viologen upon dark–light transition of *Synechocystis* expecting to induce State 2 – State 1 transition in WT cells under high intensity light. The addition of methyl viologen to the dark-acclimated cells led to rapid light-induced oxidation of P700 and intersystem electron carriers, Q_B and PQH_2 (Fig. 10), but it did not stimulate the State 2 – State 1 transition in the WT under strong illumination. It appears from these results that oxidation of intersystem electron-transport carriers may be insufficient by itself for the induction of State 2 – State 1 transition in *Synechocystis*.

The data obtained in the present and previous (Bulychev et al. 2018; Elanskaya et al. 2021) papers show that using mutants devoid of flavodiiron proteins it is possible to study in detail the processes occurring upon dark–light

transition of cyanobacteria. In the WT *Synechocystis*, the period of FNR and Calvin cycle activation upon dark–light transition is accompanied by LET, which is supported by the flavodiiron proteins Flv1/Flv3 heterodimer, accepting electrons from PSI. In the dark-acclimated Flv-deficient mutants, activation of LET upon illumination is preceded by CET that maintains State 2. LET begins earlier than the S-M rise in Chl fluorescence, and the oxidation of PQH_2 pool promotes the activation of PSII, transient re-reduction of $P700^+$ and transition to State 1. These processes may be accompanied by disconnection of PBSs from photosystems. Experiment with methyl viologen shows, that oxidation of intersystem electron-transport carriers might be insufficient for the induction of State 2 – State 1 transition in WT of cyanobacteria under high light. Confirmation of these data requires further research.

Acknowledgements The work was supported by the Russian Science Foundation (Grant Number 21-44-00005).

Author contributions All authors contributed equally.

Declarations

Conflict of interest Authors declare no conflict of interests.

References

Adir N, Bar-Zvi S, Harris D (2020) The amazing phycobilisome. Biochim Biophys Acta. https://doi.org/10.1016/j.bbabio.2019.07.002

Allahverdiyeva Y, Ermakova M, Eisenhut M, Zhang P, Richaud P, Hagemann M, Cournac L, Aro EM (2011) Interplay between flavodiiron proteins and photorespiration in *Synechocystis* sp. PCC 6803. J Biol Chem. https://doi.org/10.1074/jbc.M111.223289

Allahverdiyeva Y, Mustila H, Ermakova M, Bersanini L, Richaud P, Ajlani G, Battchikova N, Cournac L, Aro E-M (2013) Flavodiiron proteins Flv1 and Flv3 enable cyanobacterial growth and photosynthesis under fluctuating light. Proc Natl Acad Sci 110(10):4111–4116

Allahverdiyeva Y, Isojärvi J, Zhang P, Aro E-M (2015) Cyanobacterial oxygenic photosynthesis is protected by flavodiiron proteins. Life 5(1):716–743

Aro E-M, Virgin I, Andersson B (1993) Photoinhibition of Photosystem II. Inactivation, protein damage and turnover. Biochim Biophys Acta 1143(2):113–134. https://doi.org/10.1016/0005-2728(93)90134-2

Arteni AA, Ajlani G, Boekema EJ (2009) Structural organisation of phycobilisomes from *Synechocystis* sp. strain PCC6803 and their interaction with the membrane. Biochim Biophys Acta 1787(4):272–279. https://doi.org/10.1016/j.bbabio.2009.01.009

Ashby MK, Mullineaux CW (1999) The role of ApcD and ApcF in energy transfer from phycobilisomes to PS I and PS II in a cyanobacterium. Photosynthesis Res 61(2):169–179. https://doi.org/10.1023/A:1006217201666

Battchikova N, Wei L, Du L, Bersanini L, Aro EM, Ma W (2011) Identification of novel Ssl0352 protein (NdhS), essential for efficient operation of cyclic electron transport around photosystem I, in NADPH:plastoquinone oxidoreductase (NDH-1) complexes of *Synechocystis* sp. PCC 6803. J Biol Chem 286(42):36992–37001. https://doi.org/10.1074/jbc.M111.263780

Bendall DS, Manasse RS (1995) Cyclic photophosphorylation and electron transport. Biochim Biophys Acta 1229(1):23–38. https://doi.org/10.1016/0005-2728(94)00195-B

Bhatti AF, Choubeh RR, Kirilovsky D, Wientjes E, van Amerongen H (2020) State transitions in cyanobacteria studied with picosecond fluorescence at room temperature. Biochim Biophys Acta. https://doi.org/10.1016/j.bbabio.2020.148255

Bolychevtseva YV, Tropin IV, Stadnichuk IN (2021) State 1 and state 2 in photosynthetic apparatus of red microalgae and Cyanobacteria. Biochem Biokhimiia 86(10):1181–1191. https://doi.org/10.1134/s0006297921100023

Bonaventura C, Myers J (1969) Fluorescence and oxygen evolution from *Chlorella pyrenoidosa*. Biochim Biophys Acta 189(3):366–383. https://doi.org/10.1016/0005-2728(69)90168-6

Bulychev AA, Cherkashin AA, Muronets EM, Elanskaya IV (2018) Photoinduction of electron transport on the acceptor side of PSI in *Synechocystis* PCC 6803 mutant deficient in flavodiiron proteins Flv1 and Flv3. Biochim Biophys Acta 10:1086–1095. https://doi.org/10.1016/j.bbabio.2018.06.012

Calzadilla PI, Kirilovsky D (2020) Revisiting cyanobacterial state transitions. Photochem Photobiol Sci 19(5):585–603. https://doi.org/10.1039/C9PP00451C

Calzadilla PI, Muzzopappa F, Sétif P, Kirilovsky D (2019) Different roles for ApcD and ApcF in Synechococcus elongatus and *Synechocystis* sp. PCC 6803 phycobilisomes. Biochim Biophys Acta 6:488–498. https://doi.org/10.1016/j.bbabio.2019.04.004

Choubeh RR, Wientjes E, Struik PC, Kirilovsky D, van Amerongen H (2018) State transitions in the cyanobacterium *Synechococcus elongatus* 7942 involve reversible quenching of the photosystem II core. Biochim Biophys Acta (BBA)-Bioenerg. https://doi.org/10.1016/j.bbabio.2018.06.008

Chukhutsina V, Bersanini L, Aro E-M, van Amerongen H (2015) Cyanobacterial light-harvesting phycobilisomes uncouple from photosystem I during dark-to-light transitions. Sci Rep 5(1):14193. https://doi.org/10.1038/srep14193

Deng G, Liu F, Liu X, Zhao J (2012) Significant energy transfer from CpcG2-phycobilisomes to photosystem I in the cyanobacterium *Synechococcus* sp. PCC 7002 in the absence of ApcD-dependent state transitions. FEBS Lett 586(16):2342–2345. https://doi.org/10.1016/j.febslet.2012.05.038

Domínguez-Martín MA, Sauer PV, Kirst H, Sutter M, Bína D, Greber BJ, Nogales E, Polívka T, Kerfeld CA (2022) Structures of a phycobilisome in light-harvesting and photoprotected states. Nature 609(7928):835–845. https://doi.org/10.1038/s41586-022-05156-4

Dong CX, Zhao JD (2008) ApcD is required for state transition but not involved in blue-light induced quenching in the cyanobacterium *Anabaena* sp. PCC7120. Chin Sci Bull 53(21):3422–3424

Dong C, Tang A, Zhao J, Mullineaux CW, Shen G, Bryant DA (2009) ApcD is necessary for efficient energy transfer from phycobilisomes to photosystem I and helps to prevent photoinhibition in the cyanobacterium *Synechococcus* sp. PCC 7002. Biochim Biophys Acta 1787(9):1122–1128. https://doi.org/10.1016/j.bbabio.2009.04.007

El Bissati K, Delphin E, Murata N, Etienne AL, Kirilovsky D (2000) Photosystem II fluorescence quenching in the cyanobacterium *Synechocystis* PCC 6803: involvement of two different mechanisms. Biochim Biophys Acta 1457(3):229–242. https://doi.org/10.1016/S0005-2728(00)00104-3

Elanskaya IV, Bulychev AA, Lukashev EP, Muronets EM (2021) Deficiency in flavodiiron protein Flv3 promotes cyclic electron flow and state transition under high light in the cyanobacterium *Synechocystis* sp. PCC 6803. Biochim Biophys Acta. https://doi.org/10.1016/j.bbabio.2020.148318

Ermakova M, Huokko T, Richaud P, Bersanini L, Howe CJ, Lea-Smith DJ, Peltier G, Allahverdiyeva Y (2016) Distinguishing the roles

of thylakoid respiratory terminal oxidases in the cyanobacterium *Synechocystis* sp. PCC 6803. Plant Physiol 171(2):1307–1319. https://doi.org/10.1104/pp.16.00479

Fork DC, Satoh K (1983) State I-State II transitions in the thermophilic blue-green alga (Cyanobacterium) *Synechococcus lividus**. Photochem Photobiol 37(4):421–427. https://doi.org/10.1111/j.1751-1097.1983.tb04495.x

Gao F, Zhao J, Chen L, Battchikova N, Ran Z, Aro E-M, Ogawa T, Ma W (2016) The NDH-1L-PSI supercomplex is important for efficient cyclic electron transport in Cyanobacteria. Plant Physiol 172(3):1451–1464. https://doi.org/10.1104/pp.16.00585

Gerotto C, Alboresi A, Meneghesso A, Jokel M, Suorsa M, Aro E-M, Morosinotto T (2016) Flavodiiron proteins act as safety valve for electrons in *Physcomitrella patens*. Proc Natl Acad Sci 113(43):12322–12327. https://doi.org/10.1073/pnas.1606685113

Glazer AN (1984) Phycobilisome a macromolecular complex optimized for light energy transfer. Biochim Biophys Acta (BBA) - Rev Bioenerg 768(1):29–51. https://doi.org/10.1016/0304-4173(84)90006-5

Golub M, Moldenhauer M, Schmitt F-J, Feoktystov A, Mändar H, Maksimov E, Friedrich T, Pieper J (2019a) Solution structure and conformational flexibility in the active state of the orange carotenoid protein: part I. Small-angle scattering. J Phys Chem B 123(45):9525–9535. https://doi.org/10.1021/acs.jpcb.9b05071

Golub M, Moldenhauer M, Schmitt F-J, Lohstroh W, Maksimov EG, Friedrich T, Pieper J (2019b) Solution structure and conformational flexibility in the active state of the orange carotenoid protein part II: quasielastic neutron scattering. J Phys Chem B 123(45):9536–9545. https://doi.org/10.1021/acs.jpcb.9b05073

Govindjee E (1995) 63 years since Kautsky-chlorophyll-a fluorescence. Aust J Plant Physiol 22(2):131–160

Gwizdala M, Wilson A, Kirilovsky D (2011) In vitro reconstitution of the Cyanobacterial photoprotective mechanism mediated by the orange carotenoid protein in *Synechocystis* PCC 6803. Plant Cell 23(7):2631–2643. https://doi.org/10.1105/tpc.111.086884

Hanke GT, Satomi Y, Shinmura K, Takao T, Hase T (2011) A screen for potential ferredoxin electron transfer partners uncovers new, redox dependent interactions. Biochim Biophys Acta 2:366–374. https://doi.org/10.1016/j.bbapap.2010.09.011

Helman Y, Tchernov D, Reinhold L, Shibata M, Ogawa T, Schwarz R, Ohad I, Kaplan A (2003) Genes encoding A-type flavoproteins are essential for photoreduction of O_2 in cyanobacteria. Curr Biol 13(3):230–235. https://doi.org/10.1016/s0960-9822(03)00046-0

Huang W, Quan X, Zhang S-B, Liu T (2018) In vivo regulation of proton motive force during photosynthetic induction. Environ Exp Bot 148:109–116. https://doi.org/10.1016/j.envexpbot.2018.01.001

Huang W, Yang Y-J, Zhang S-B (2019a) Photoinhibition of photosystem I under fluctuating light is linked to the insufficient ΔpH upon a sudden transition from low to high light. Environ Exp Bot 160:112–119

Huang W, Yang Y-J, Zhang S-B (2019b) The role of water-water cycle in regulating the redox state of photosystem I under fluctuating light. Biochim Biophys Acta 5:383–390. https://doi.org/10.1016/j.bbabio.2019.03.007

Ilík P, Pavlovič A, Kouřil R, Alboresi A, Morosinotto T, Allahverdiyeva Y, Aro EM, Yamamoto H, Shikanai T (2017) Alternative electron transport mediated by flavodiiron proteins is operational in organisms from cyanobacteria up to gymnosperms. New Phytol 214(3):967–972. https://doi.org/10.1111/nph.14536

Jokel M, Johnson X, Peltier G, Aro EM, Allahverdiyeva Y (2018) Hunting the main player enabling *Chlamydomonas reinhardtii* growth under fluctuating light. Plant J 94(5):822–835. https://doi.org/10.1111/tpj.13897

Kaňa R, Kotabová E, Komárek O, Šedivá B, Papageorgiou GC, Prášil O (2012) The slow S to M fluorescence rise in cyanobacteria is due to a state 2 to state 1 transition. Biochim Biophys Acta. https://doi.org/10.1016/j.bbabio.2012.02.024

Kirilovsky D, Kerfeld CA (2012) The orange carotenoid protein in photoprotection of photosystem II in cyanobacteria. Biochim Biophys Acta 1:158–166. https://doi.org/10.1016/j.bbabio.2011.04.013

Kramer M, Rodriguez-Heredia M, Saccon F, Mosebach L, Twachtmann M, Krieger-Liszkay A, Duffy C, Knell RJ, Finazzi G, Hanke GT (2021) Regulation of photosynthetic electron flow on dark to light transition by ferredoxin:NADP(H) oxidoreductase interactions. Elife. https://doi.org/10.7554/eLife.56088

Kuzminov F, Bolychevtseva YV, Elanskaya I, Karapetyan N (2014) Effect of APCD and APCF subunits depletion on phycobilisome fluorescence of the cyanobacterium *Synechocystis* PCC 6803. J Photochem Photobiol B: Biol 133:153–160

Laisk A, Eichelmann H, Oja V, Rasulov B, Padu E, Bichele I, Pettai H, Kull O (2005) Adjustment of leaf photosynthesis to shade in a natural canopy: rate parameters. Plant, Cell Environ 28(3):375–388. https://doi.org/10.1111/j.1365-3040.2004.01274.x

Leverenz RL, Sutter M, Wilson A, Gupta S, Thurotte A, Bourcier de Carbon C, Petzold CJ, Ralston C, Perreau F, Kirilovsky D, Kerfeld CA (2015) A 12 Å carotenoid translocation in a photoswitch associated with cyanobacterial photoprotection. Science 348(6242):1463–1466. https://doi.org/10.1126/science.aaa7234

Mattila H, Khorobrykh S, Hakala-Yatkin M, Havurinne V, Kuusisto I, Antal T, Tyystjärvi T, Tyystjärvi E (2020) Action spectrum of the redox state of the plastoquinone pool defines its function in plant acclimation. Plant J 104(4):1088–1104. https://doi.org/10.1111/tpj.14983

McConnell MD, Koop R, Vasil'ev S, Bruce D (2002) Regulation of the distribution of chlorophyll and phycobilin-absorbed excitation energy in cyanobacteria. A structure-based model for the light state transition. Plant Physiol 130(3):1201–1212. https://doi.org/10.1104/pp.009845

Miller NT, Vaughn MD, Burnap RL (2021) Electron flow through NDH-1 complexes is the major driver of cyclic electron flow-dependent proton pumping in cyanobacteria. Biochim Biophys Acta Bioenerg. https://doi.org/10.1016/j.bbabio.2020.148354

Minagawa J (2011) State transitions–the molecular remodeling of photosynthetic supercomplexes that controls energy flow in the chloroplast. Biochim Biophys Acta 1807(8):897–905. https://doi.org/10.1016/j.bbabio.2010.11.005

Mullineaux C (2014) Electron transport and light-harvesting switches in cyanobacteria. Front Plant Sci. https://doi.org/10.3389/fpls.2014.00007

Mullineaux CW, Allen JF (1990) State 1-state 2 transitions in the cyanobacterium *Synechococcus* 6301 are controlled by the redox state of electron carriers between Photosystems I and II. Photosynthesis Res 23(3):297–311. https://doi.org/10.1007/BF00034860

Mullineaux CW, Emlyn-Jones D (2004) State transitions: an example of acclimation to low-light stress. J Exp Bot 56(411):389–393. https://doi.org/10.1093/jxb/eri064

Munekage Y, Hashimoto M, Miyake C, Tomizawa K-I, Endo T, Tasaka M, Shikanai T (2004) Cyclic electron flow around photosystem I is essential for photosynthesis. Nature 429(6991):579–582. https://doi.org/10.1038/nature02598

Mustila H, Paananen P, Battchikova N, Santana-Sánchez A, Muth-Pawlak D, Hagemann M, Aro E-M, Allahverdiyeva Y (2016) The flavodiiron protein Flv3 functions as a homo-oligomer during stress acclimation and is distinct from the Flv1/Flv3 hetero-oligomer specific to the O_2 photoreduction pathway. Plant Cell Physiol 57(7):1468–1483. https://doi.org/10.1093/pcp/pcw047

Nikkanen L, Santana Sánchez A, Ermakova M, Rögner M, Cournac L, Allahverdiyeva Y (2020) Functional redundancy between

flavodiiron proteins and NDH-1 in *Synechocystis* sp. PCC 6803. Plant J 103(4):1460–1476. https://doi.org/10.1111/tpj.14812

Noridomi M, Nakamura S, Tsuyama M, Futamura N, Vladkova R (2017) Opposite domination of cyclic and pseudocyclic electron flows in short-illuminated dark-adapted leaves of angiosperms and gymnosperms. Photosynthesis Res 134(2):149–164. https://doi.org/10.1007/s11120-017-0419-2

Papageorgiou GC, Tsimilli-Michael M, Stamatakis K (2007) The fast and slow kinetics of chlorophyll a fluorescence induction in plants, algae and cyanobacteria: a viewpoint. Photosynth Res 94(2–3):275–290. https://doi.org/10.1007/s11120-007-9193-x

Peden EA, Boehm M, Mulder DW, Davis R, Old WM, King PW, Ghirardi ML, Dubini A (2013) Identification of global ferredoxin interaction networks in *Chlamydomonas reinhardtii*. J Biol Chem 288(49):35192–35209. https://doi.org/10.1074/jbc.M113.483727

Peltier G, Aro EM, Shikanai T (2016) NDH-1 and NDH-2 plastoquinone reductases in oxygenic photosynthesis. Annu Rev Plant Biol 67:55–80. https://doi.org/10.1146/annurev-arplant-043014-114752

Protasova EA, Antal TK, Zlenko DV, Elanskaya IV, Lukashev EP, Friedrich T, Mironov KS, Sluchanko NN, Ge B, Qin S, Maksimov EG (2021) State of the phycobilisome determines effective absorption cross-section of Photosystem II in *Synechocystis* sp. PCC 6803. Biochim Biophys Acta. https://doi.org/10.1016/j.bbabio.2021.148494

Ranjbar Choubeh R, Wientjes E, Struik PC, Kirilovsky D, Amerongen H, van (2018) State transitions in the cyanobacterium Synechococcus elongatus 7942 involve reversible quenching of the photosystem II core. Biochim Biophys Acta 10:1059–1066. https://doi.org/10.1016/j.bbabio.2018.06.008

Saha R, Liu D, Hoynes-O'Connor A, Liberton M, Yu J, Bhattacharyya-Pakrasi M, Balassy A, Zhang F, Moon TS, Maranas CD, Pakrasi HB (2016) Diurnal regulation of cellular processes in the Cyanobacterium *Synechocystis* sp. strain PCC 6803 insights from transcriptomic, fluxomic, and physiological analyses. Mbio 7(3):e00464-e1416. https://doi.org/10.1128/mBio.00464-16

Schansker G, Tóth SZ, Strasser RJ (2005) Methylviologen and dibromothymoquinone treatments of pea leaves reveal the role of photosystem I in the Chl a fluorescence rise OJIP. Biochim Biophys Acta 1706(3):250–261. https://doi.org/10.1016/j.bbabio.2004.11.006

Schreiber U, Klughammer C (2021) Evidence for variable chlorophyll fluorescence of photosystem I in vivo. Photosynthesis Res 149(1):213–231. https://doi.org/10.1007/s11120-020-00814-y

Schuller JM, Birrell JA, Tanaka H, Konuma T, Wulfhorst H, Cox N, Schuller SK, Thiemann J, Lubitz W, Sétif P, Ikegami T, Engel BD, Kurisu G, Nowaczyk MM (2019) Structural adaptations of photosynthetic complex I enable ferredoxin-dependent electron transfer. Science 363(6424):257–260. https://doi.org/10.1126/science.aau3613

Sétif P, Shimakawa G, Krieger-Liszkay A, Miyake C (2020) Identification of the electron donor to flavodiiron proteins in *Synechocystis* sp. PCC 6803 by in vivo spectroscopy. Biochim Biophys Acta. https://doi.org/10.1016/j.bbabio.2020.148256

Stadnichuk IN, Lukashev EP, Elanskaya IV (2009) Fluorescence changes accompanying short-term light adaptations in photosystem I and photosystem II of the cyanobacterium *Synechocystis* sp. PCC 6803 and phycobiliprotein-impaired mutants: state 1/state 2 transitions and carotenoid-induced quenching of phycobilisomes. Photosynth Res 99(3):227–241. https://doi.org/10.1007/s11120-009-9402-x

Stirbet A, Lazár D, Papageorgiou GC (2019) Chapter 5 - Chlorophyll a Fluorescence in Cyanobacteria: Relation to Photosynthesis. In: Mishra AK, Tiwari DN, Rai AN (eds) Cyanobacteria. Academic Press, Cambridge, pp 79–130. https://doi.org/10.1016/B978-0-12-814667-5.00005-2

Tamoi M, Shigeoka S (2015) Diversity of regulatory mechanisms of photosynthetic carbon metabolism in plants and algae. Biosci Biotechnol Biochem 79(6):870–876. https://doi.org/10.1080/09168451.2015.1020754

Tamoi M, Miyazaki T, Fukamizo T, Shigeoka S (2005) The Calvin cycle in cyanobacteria is regulated by CP12 via the NAD(H)/NADP(H) ratio under light/dark conditions. Plant J 42(4):504–513. https://doi.org/10.1111/j.1365-313X.2005.02391.x

Vicente JB, Gomes CM, Wasserfallen A, Teixeira M (2002) Module fusion in an A-type flavoprotein from the cyanobacterium *Synechocystis* condenses a multiple-component pathway in a single polypeptide chain. Biochem Biophys Res Commun 294(1):82–87. https://doi.org/10.1016/s0006-291x(02)00434-5

Wada S, Yamamoto H, Suzuki Y, Yamori W, Shikanai T, Makino A (2018) Flavodiiron protein substitutes for cyclic electron flow without competing CO(2) assimilation in rice. Plant Physiol 176(2):1509–1518. https://doi.org/10.1104/pp.17.01335

Wilson A, Ajlani G, Verbavatz JM, Vass I, Kerfeld CA, Kirilovsky D (2006) A soluble carotenoid protein involved in phycobilisome-related energy dissipation in cyanobacteria. Plant Cell 18(4):992–1007. https://doi.org/10.1105/tpc.105.040121

Yamamoto H, Takahashi S, Badger MR, Shikanai T (2016) Artificial remodelling of alternative electron flow by flavodiiron proteins in Arabidopsis. Nature Plants 2(3):16012. https://doi.org/10.1038/nplants.2016.12

Yamori W (2016) Photosynthetic response to fluctuating environments and photoprotective strategies under abiotic stress. J Plant Res 129(3):379–395. https://doi.org/10.1007/s10265-016-0816-1

Yamori W, Shikanai T (2016) Physiological functions of cyclic electron transport around photosystem I in sustaining photosynthesis and plant growth. Annu Rev Plant Biol 67:81–106. https://doi.org/10.1146/annurev-arplant-043015-112002

Yaroshevich IA, Maksimov EG, Sluchanko NN, Zlenko DV, Stepanov AV, Slutskaya EA, Slonimskiy YB, Botnarevskii VS, Remeeva A, Gushchin I, Kovalev K, Gordeliy VI, Shelaev IV, Gostev FE, Khakhulin D, Poddubnyy VV, Gostev TS, Cherepanov DA, Polívka T, Kloz M, Friedrich T, Paschenko VZ, Nadtochenko VA, Rubin AB, Kirpichnikov MP (2021) Role of hydrogen bond alternation and charge transfer states in photoactivation of the orange carotenoid protein. Commun Biol 4(1):539. https://doi.org/10.1038/s42003-021-02022-3